INFORMATION TO USERS

This manuscript has been reproduced from the microfilm master. UMI films the text directly from the original or copy submitted. Thus, some thesis and dissertation copies are in typewriter face, while others may be from any type of computer printer.

The quality of this reproduction is dependent upon the quality of the copy submitted. Broken or indistinct print, colored or poor quality illustrations and photographs, print bleedthrough, substandard margins, and improper alignment can adversely affect reproduction.

In the unlikely event that the author did not send UMI a complete manuscript and there are missing pages, these will be noted. Also, if unauthorized copyright material had to be removed, a note will indicate the deletion.

Oversize materials (e.g., maps, drawings, charts) are reproduced by sectioning the original, beginning at the upper left-hand corner and continuing from left to right in equal sections with small overlaps. Each original is also photographed in one exposure and is included in reduced form at the back of the book.

Photographs included in the original manuscript have been reproduced xerographically in this copy. Higher quality 6" x 9" black and white photographic prints are available for any photographs or illustrations appearing in this copy for an additional charge. Contact UMI directly to order.

UMI

A Bell & Howell Information Company
300 North Zeeb Road, Ann Arbor MI 48106-1346 USA
313/761-4700 800/521-0600

A Physical Characterization of Eucaryotic Initiation Factor 4E

By

Diana Friedland

A dissertation submitted to the Graduate Faculty in Chemistry in partial fulfillment of the requirements for the degree of Doctor of Philosophy, The City University of New York.

1999

This manuscript has been read and accepted for the Graduate Faculty in Chemistry in satisfaction of the dissertation requirement for the degree of Doctor of Philosophy.

1/21/99
Date

Chair of Examining Committee

1-28-99
Date

Professor Gerald Koppel/UKM
Executive Officer

Supervisory Committee

The City University of New York

Abstract

A Physical Characterization of Eucaryotic Initiation Factor 4E

By

Diana Friedland

Advisor: Professor Dixie J. Goss

A characterization of eIF-4E was achieved using several techniques. Identification of the amino acid residues involved in the eukaryotic mRNA cap binding domain of mammalian eIF-4E was achieved using the photoaffinity analogue [γ-^{32}P]8-N_3GTP. Amino acid sequencing identified the binding domain as the region containing the sequence Trp 113-Arg 122. Lys 119 was not identified in sequencing analysis nor was it cleaved by trypsin. These results indicate that Lys 119 is the residue directly modified by photoinsertion of [γ-^{32}P]8-N_3GTP. Direct fluorescence techniques were used to measure the equilibrium constant of the recombinant eIF-4E used in this study. This was done in order to confirm that the recombinant protein had biological and physical characteristics that are similar or identical to native eIF-4E. This information was used to synthesize a peptide consisting of the eIF-4E binding site domain. Fluorescence measurements were used to

determine the equilibrium activity of the peptide which was two orders of magnitude greater than that of the native, intact protein. The peptide was then used for the purpose of developing an affinity peptide column for use in isolating globin mRNA. To further identify the significance of these amino acids in mRNA cap binding and to determine their functional roles, fluorescence and circular dichroism studies were performed on ,eIF-4E in which the individual amino acids between Arg 112 and Gln 121 were mutated to alanine. The analyses of these mutant proteins indicates that mutants of eIF-4E of varying cap affinity can be engineered.

Acknowledgements

I would like to thank the people who have encouraged and supported me throughout this work. I thank Dr. Dixie Goss, my advisor and friend who showed confidence in me and my abilities and who gave me the tools to make this work possible. I thank my committee members: Dr Lynn Francesconi from Hunter College, Dr. Robert Callender and Dr. Marilyn Gunner from City College, and my close advisor Dr. Boyd Haley from the University of Kentucky Medical Center. To my husband Sebastian McClendon who patiently supported and helped me through this writing process. To my father, Doug and to my family who have shown unwavering support for me all these years. To my late husband Michael Cohen who believed that I was capable of achieving anything I wanted to do in life and made me believe it too. Lastly I thank Dr. Luisa M. Balasta, Dr. Curt H. Hagedorn, Susie Boydston-White and Dr. Michael T. Shoemaker for all of their help and advice.

I acknowledge the financial support I have received throughout my doctoral education:

National Science Foundation (DGE-9553549)

Glaxo-Wellcome Company (Gertrude Elion Fellowship)

Helen Samuels Schectman Scholarship

Mina Reese Scholarship

Robert E. Gilleece Fellowship

Table of Contents

Abbreviations

m^7GTP	7-methyl guanosine triphosphate
eIF	eukaryotic initiation factor
$_r$eIF	recombinant eukaryotic initiation factor
DTT	dithiothreitol
TFA	tri-fluoro acetic acid
TCA	tri-chloro acetic acid
PTH	phenylthiohydantoin
8-N_3GTP	8-azidoguanosine 5'-triphosphate
FPLC	fast protein liquid chromatography
HPLC	high pressure liquid chromatography
Tris	tris(hydroxymethyl)aminomethane
HEPES	N-(2-hydroxyethyl)piperazine-N'-2-ethanesulfonic acid
kDa	kilodalton

List of Tables

List of Figures

Chapter 1

Introduction

Overview of eIF-4E's Role In Protein Synthesis

Protein synthesis is divided into three phases: initiation; elongation; and termination. Because this thesis will be dealing with the initiation phase, I will only briefly mention the last two phases. Elongation involves the binding of an aminoacyl-tRNA, carrying a carboxy-linked amino acid to the ribosome. Peptide bond formation occurs during this stage. The termination phase occurs when a stop signal on the mRNA (usually UAA, UGA, or UAG) is recognized by protein release factors thus releasing the completed polypeptide chain from the ribosome. This occurs because tRNAs do not contain anticodons which recognize these signals. The initiation phase of eukaryotic protein synthesis is characterized by recognition of the m^7(5')Gppp(5')N, (where N is any nucleotide), cap structure at the 5' terminus of eukaryotic mRNA by initiation factors and is an incredibly complex process involving dozens of proteins, reviewed in references (Rhoads, 1988, Sonenberg, 1996). The initiation phase itself is also characterized by three steps: (1) formation of the 43S initiation complex; (2) formation of the 48S initiation complex which consists of mRNA binding to the 43S complex and subsequent scanning for the initiation codon; and (3) formation of the 80S initiation complex (Rhoads, 1988), (Fig. 1). In spite of the fact that the initiation factors involved have indeed been identified, the biochemical processand molecular model of initiation remain unclear. Of the eIF's which interact at or near the cap it has been shown that only eIF-4E (alone or as part of the eIF-4F complex) interacts directly with the cap (Grifo et al., 1983, Hellman et al., 1982, Sonenberg, 1981, Tahara et al., 1981, Webb et al., 1984). However

Figure 1. A model for the formation of the 48S initiation complex. Rhoads, R.E. (1988). TIBS **13**: 52-56.

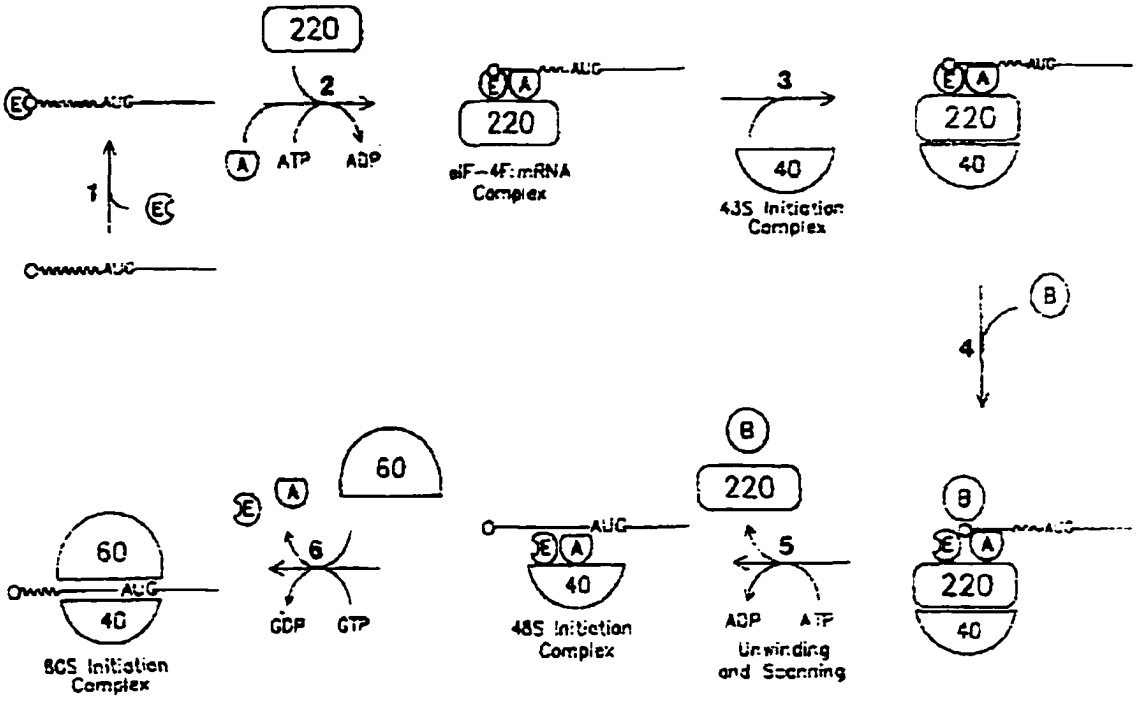

4E does not act alone in mammalian systems but rather as part of the eIF-4F, a tri-mer protein complex also consisting of eIF-4A and eIF-4G (also known as p220) (Merrick & Hershey, 1996). Additionally eIF-4B is required for mRNA binding, see Fig. 2. eIF-4A is an RNA helicase that is suspected to be responsible for the unwinding of the secondary structure in the 5' untranslated region of mRNA (Abramson et al., 1987, Rozen et al., 1990). 4A shares a sequence motif similar to that of other proteins which have been found to have known helicase activity. Additionally it possesses RNA-dependent ATPase activity (Abramson et al., 1987). It has recently been revealed that eIF-4G serves as a molecular bridge between 4E and 4A, with 4E binding to the amino-terminus of 4G and 4A binding to the carboxy-terminus (Lamphear et al., 1995, Mader et al., 1995) (Fig. 3). This initial recognition of the cap structure represents the first committed step in the initiation phase of protein synthesis. Translation initiation, which involves recognition of the capped mRNA, binding of the ribosomal subunits, and selection of the start codon, is generally considered to be the limiting phase of translation (Pain, 1996). Evidence that cap recognition by eIF-4E is itself a limiting step in protein synthesis is supported by the observation that it is the least abundant of all the initiation factors and thus may serve a regulatory function (Duncan et al., 1987). In keeping with this it has previously been determined that 4E is present at only 2-5% the molar concentration of ribosomes (Hiremath et al., 1985).

In addition, there are a number of other observations indicating that eIF-4E is a key point for post-transcriptional control of gene expression. They include: the rapid stimulation of

Figure 2. Model for the mechanism of action of mRNA-binding initiation factors. The steps leading to ribosome binding are (1) binding of eIF-4F to the cap structure of the mRNA, followed by the binding of eIF-4B, (2) unwinding of the proximal mRNA 5' secondary structure in an ATP-dependent manner, and (3) recycling of eIF-4A through the eIF-4F complex. Sonenberg, S. (1996). Translational Control 245-269.

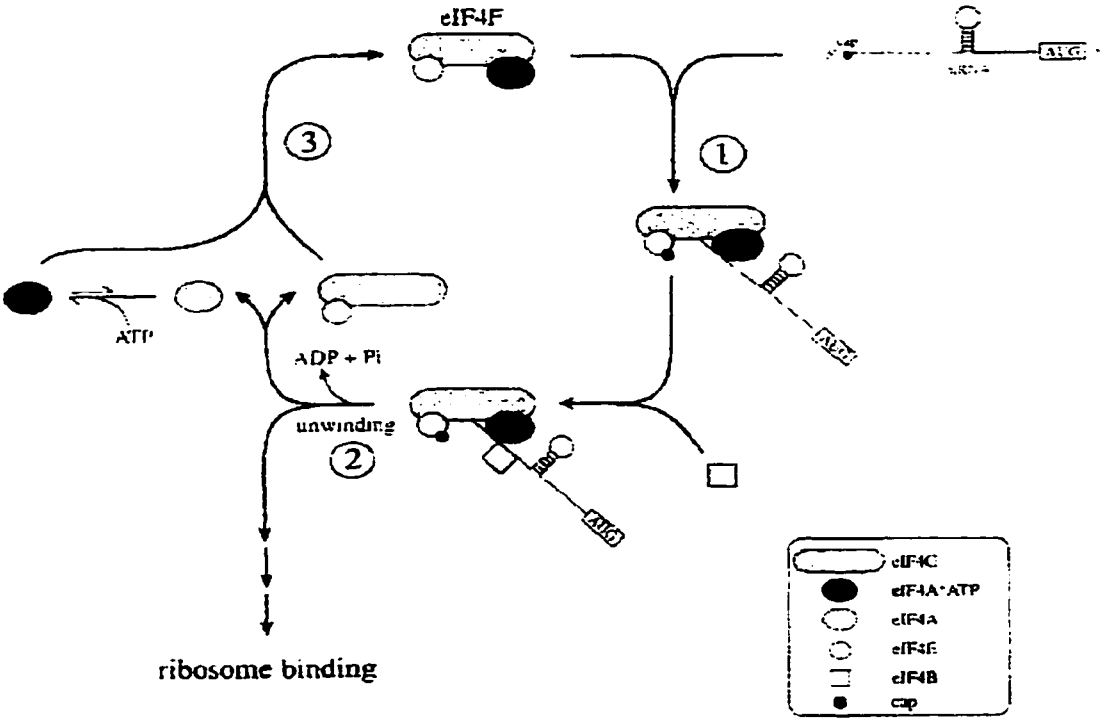

Figure 3. Model for eIF-4G serving as a bridge between eIF-4E and the helicase eIF-4A, which melts secondary structure in the mRNA. This allows more efficient binding and/or scanning by the 40S ribosomal subunit. Lawrence, J.C. and Abraham, R.T. (1997). TIBS **22** 345-349.

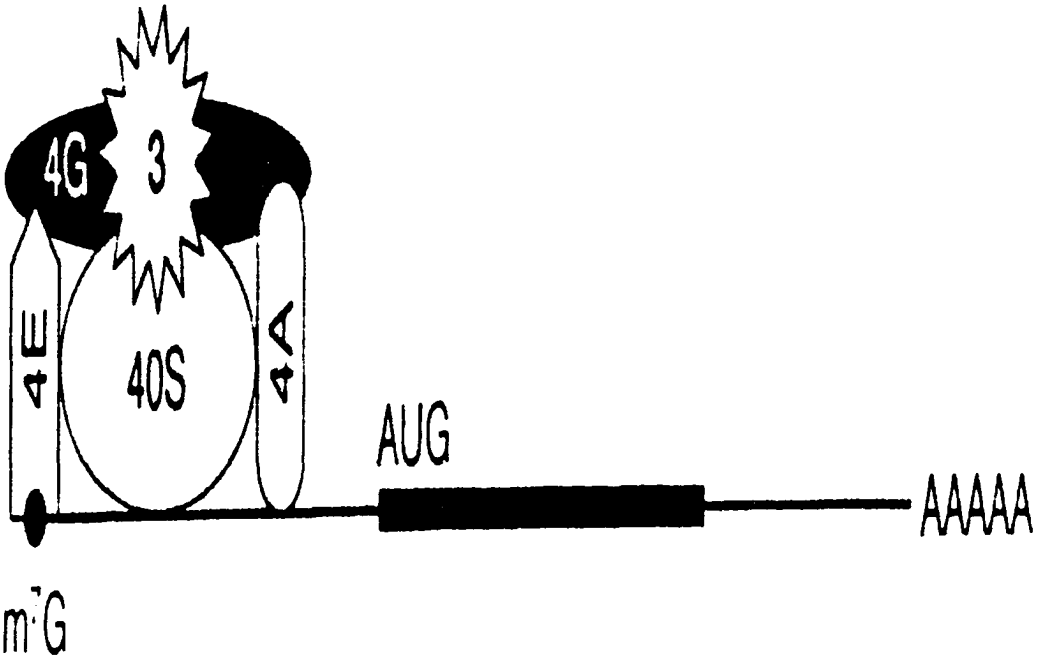

eIF-4E phosphorylation by epidermal growth factor and other growth regulatory peptides in intact cells (Donaldson et al., 1991, Proud, 1992, Rhoads, 1993, Sonnenberg, 1994). Indeed, when 4E is over expressed it behaves as an oncogene (Lazaris-Karantzas et al., 1990). Abnormally high levels of 4E have been detected in a number of transformed cell lines and breast carcinomas (Miyage et al., 1995). Also, there is evidence from two different cellular systems that hyperphosphorylation of eIF-4E promotes the recruitment of other eIF-4F subunits to the m^7G mRNA cap (Morley et al., 1993, Bu, 1993 #41); and a 3-4 fold increase in the affinity of eIF-4E binding to mRNA caps (Minich et al., 1994). Due to this modification, phosphorylated eIF-4E is highly enriched in ribosomes bound to mRNA (Joshe et al., 1994). The regulation of eIF-4E function has been shown to be even more complicated by the identification of eIF-4E binding proteins (4E-BP's) that are regulated physiologically by reversible phosphorylation, insulin, various drugs, viral infection, etc. (Lin et al., 1994, Sachs, 1997 #53). When bound to eIF-4E these proteins inhibit initiation of protein synthesis (Figs. 4 and 5). To understand fully the mechanisms by which these covalent modifications and translational repressor 4E binding proteins exert their effects, a more detailed understanding of eIF-4E structure and binding site sequence will be required.

The amino acid sequence for the cap binding protein has been previously reported for several species including yeast (Altmann & Trachsel, 1989), wheat (Metx et al., 1992), human (Rychlik et al., 1987), and mouse (Altmann & Trachsel, 1989). The numbers and positions of the eight tryptophans are highly conserved with there being one additional tryptophan residue in p26

Figure 4. Cap-Stimulated Translation Initiation. (A) eIF-4E recruits the 40S subunit to the mRNA via a network of protein interactions. (B) Phosphorylation regulates the activity of the eIF-4E/eIF-4G complex. The effects of phosphorylation on the association of 4EBP's with eIF-4E, and on the affinity of eIF-4E for eIF-4G and the cap structure are shown. Sachs, A.B. *et al.* (1997). Cell **89** 831-838.

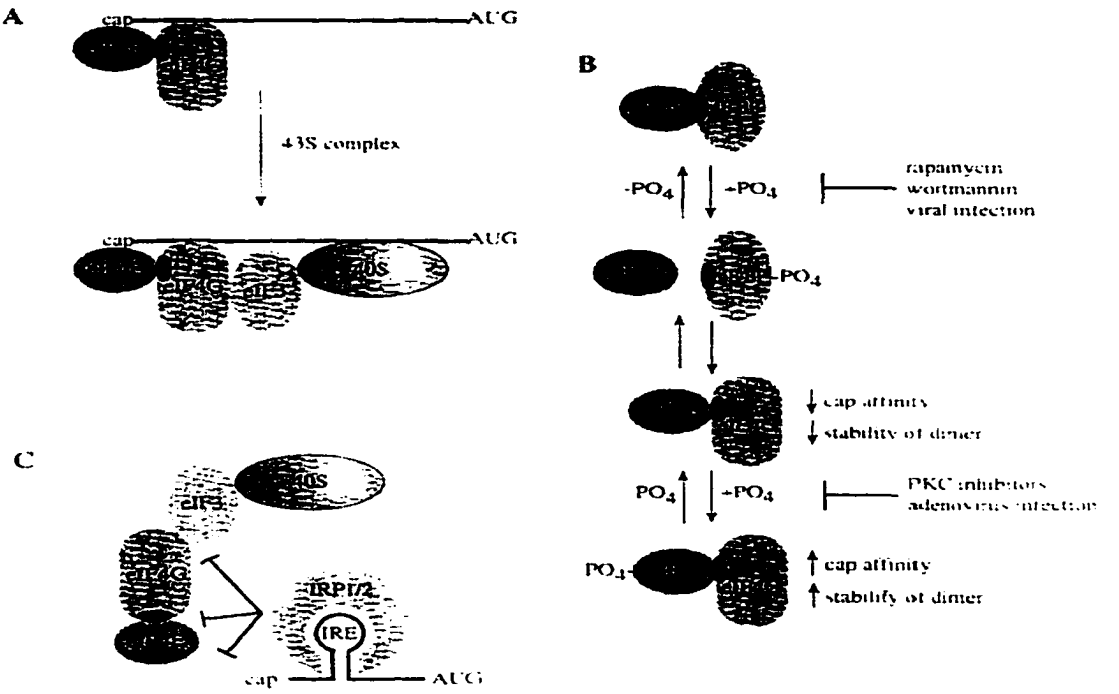

Figure 5. A model for the mechanism of stimulation of translation by insulin. The model presumes that binding of 4E-BP1 to eIF-4E prevents the interaction of the latter with p220. Insulin-dependent phosphorylation of 4E-BP1 releases eIF-4E, thus making it available to form an active cap-binding complex (eIF-4F). Pause, A., *et al.* (1994). Nature **371** 762-767.

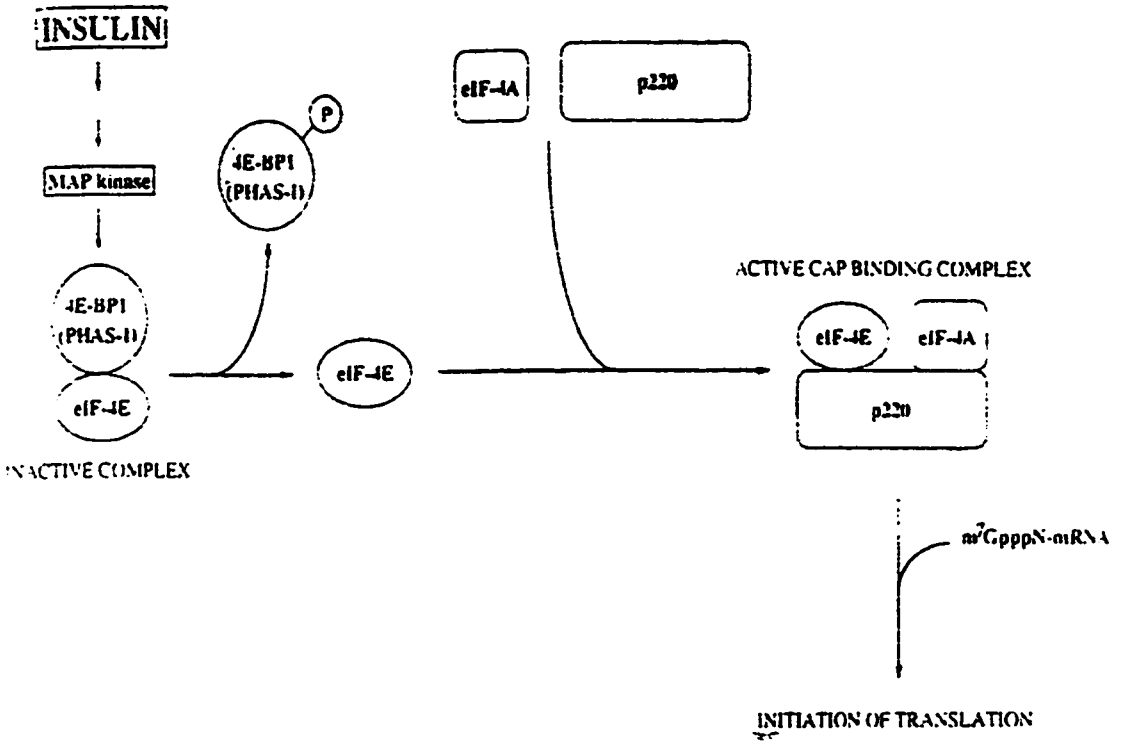

of wheat germ eIF-4F (see Table 1). Previous photoaffinity labeling of eIF-4E narrowed the active site domain to 63% of the amino acid residues (Chavan et al., 1990). Furthermore, mutational analysis suggested that a glutamic acid residue, which is located three amino acid residues to the carboxy side of tryptophan 5, participates in the binding of the mRNA cap to human eIF-4E via direct hydrogen bond formation with the 2-amino group of the m^7G base (Ueda et al., 1991b, Ueda et al., 1991a). Others proposed that a glutamic acid residue two amino acid residues to the carboxy side of tryptophan 7 participates in this hydrogen bond interaction (Koch et al., 1988, Ueda et al., 1988). However, the cap binding subunit of wheat germ eIF-4F lacks any such acidic residue in these regions (Metx et al., 1992). These conflicting results and the lack of structural information indicated the need for a more precise localization of the eIF-4E binding site for the 5' m^7G cap of mRNAs.

Photoaffinity labeling of nucleotide binding sites has provided a highly selective method for identifying the participating amino acids of many proteins (Jayaram & Haley, 1994, Salvucci et al., 1992, Shoemaker & Haley, 1993). Photoactivation of the azido moiety with ultra-violet light results in the generation of a nitrene and the subsequent covalent attachment of the probe to the binding domain through the remaining nitrogen (Potter & Haley, 1983). Immobilized aluminum(III)-chelate chromatography has facilitated the isolation of binding site peptides due to the presence of highly charged phosphates on the photoinserted azidonucleotide which interact with the Al^{3+} (Anderssen, 1991, Jayaram & Haley, 1994, Salvucci et al., 1992, Shoemaker & Haley, 1993).

Table 1. Amino acid sequence of eukaryotic initiation factor 4E. The eight tryptophans and the location of the binding site peptide are highlighted in bold.

Amino Acid Sequence of Human eIF-4E

MATVEPETTP TPNPPTTEEE KTESNQEVAN

PEHYIKHPLQ NR**W**AL**W**FFKN DKSKT**W**QANL

RLISKFDTVE DF**W**ALYNHIQL SSNLMPGCD

YSLFKDGIEP M**W**EDEKNNRG GR**WLITLNKQ**

QRRSDLDRF WLETLLCLIGE SFDDYSDDVC

GAVVNVRAK GDKIAI**W**TTEC ENREAVTHIG

RVYKERLGF PPKIVIGYQSH ADTATKSGST

TKNRFVV

Sequence 217 AA

MW 25,117

Reference Rychlik, W., Domier, L.L., Gardner, P.R., Hellmann, G.M., and Rhoads, R.E. (1987) *Proc. Natl. Acad. Sci. U.S.A.* **84**, 945-949.

[γ-^{32}P]8-N_3GTP was used to selectively label the m^7GTP cap binding domain of human recombinant eIF-4E ($_r$eIF-4E). The photolabeled peptide resulting from proteolysis was isolated using aluminum(III)-chelate chromatography followed by reversed-phase high performance liquid chromatography. The amino acid sequence of this peptide was determined and is reported here.

Chapter 2

Materials and Methods

Materials

Sequencing grade modified trypsin was obtained from Boehringer Mannheim Biochemica (Indianapolis, Indiana). Electrophoresis reagents were from Bio-Rad (Melville, New York). HPLC reagents were from E.M. Science (Gibbstown, New Jersey). All other reagents were obtained from Sigma Chemical Company (St. Louis, Missouri) and were molecular biology grade unless otherwise noted. The eIF-4E binding site peptide was synthesized by Genosys Biotechnologies (Woodlands, Texas). Agarose beads (AminoLink Plus Immobilization Kit) were purchased from Pierce Chemical Company (Rockford, IL). DNA DipStick Kit, version 3.2 was purchased from Invitrogen (San Diego, CA). Globin mRNA and uncapped mRNA were generously supplied by Life Technologies, Inc., Rockville, Maryland.

Methods

Synthesis of Photoaffinity Probe: The radioactive probe [γ-^{32}P]8-N_3GTP (specific activity, 21 mCi/μmol) was synthesized and purified as reported previously (Potter & Haley, 1983).

Recombinant eIF-4E: Expression and purification of functional $_r$eIF-4E$_{human}$ was previously described (Hagedorn et al., 1997). Mutagenesis of the binding site amino acids was performed as described (Spivak-Kroizman et al., Submitted).

Expression and Purification of eIF-4E Binding Site Mutants: Expression and purification

of eIF-4E binding site mutants was performed as described in (Spivak-Kroizman et al., Submitted).

Photoaffinity Labeling of $_r$eIF-4E: To demonstrate saturation effects, samples containing 4 μg of $_r$eIF-4E in photolysis buffer (10 mM Tris•Cl, no salt, no DTT, pH 7.6), were incubated at 4 °C in 1.5 ml Eppendorf tubes with the appropriate concentration of [γ-^{32}P]8-N_3GTP for 60 seconds. The reaction mixture was then irradiated for 90 s from a distance of 1 cm with a hand held 254 nm UVB UV lamp (intensity, 1400 μW/cm^2). The total reaction volume was 50 μl. The reaction was quenched by the addition of 250 μl of cold acetone. The sample was kept at 4 °C for 3 hours and then centrifuged in a Savant HSC10K high speed centrifuge at 10,000 rpm for 20 minutes. The supernatant was drawn off and the pellet was resuspended in a protein solubilizing mixture (PSM) consisting of 10% SDS, 3.6 M urea, 2.5% (w/v) DTT, 2% (w/v) pyronin Y (tracking dye), and 20 mM Tris•Cl (pH 8.0). For studies of protection against photoinsertion, 4 μg of $_r$eIF-4E were incubated in photolysis buffer for 60 s at 4 °C with the required competitor. At 60 s 40 μM [γ-^{32}P]8-N_3GTP was added and at 60 s the samples were irradiated, precipitated, and solubilized as described above.

SDS-PAGE, Scintillation, and Radioisotopic Imaging and Quantitation: Following solubilization, photolabeled samples were analyzed by SDS-PAGE according to the method of Laemmli (Laemmli, 1970). The gels were fixed in 25% isopropanol 10% acetic acid for one hour with frequent changes of fixing solution and dried at 80 °C on a Bio-Rad Model

583 slab gel dryer. ^{32}P incorporation into ,eIF-4E was determined with an Ambis 4000 radioisotopic imaging and quantitation system (Scanalytics/CSPI, Billerica, MA).

Photoaffinity Labeling and Enzymatic Digestion of ,eIF-4E for Binding Domain Peptide Isolation: ,eIF-4E (5 mg) was photolabeled with 50 μM [γ-^{32}P]8-N_3GTP in a 4 ml total volume of photolysis buffer. The reaction mixture was incubated at 4 °C for 5 minutes in a plastic weighing boat followed by irradiation for 2 minutes. This was followed by a second incubation and irradiation with non-radioacitve 8-N_3GTP under identical conditions. The reaction was quenched and the protein precipitated by the addition of 4 ml of cold acetone followed by incubation at 4 °C for 3 hours. The sample was collected by centrifugation for 20 minutes at 10,000 rpm. The pellet was resuspended in 2 ml of 2 M urea in 75 mM NH_4HCO_3 and the pH adjusted to 8.5-9.0 by the addition of concentrated NH_4OH. ,eIF-4E was proteolyzed by the addition of modified trypsin (10% w/v), with shaking overnight at 20 °C.

Immobilized Aluminum(III)-Chelate Chromatography: Iminodiacetic acid-epoxy-activated Sepharose (2 ml) was placed into a 15 ml centrifuge tube and washed as follows: 3 x 10 ml distilled water, 4 x 10 ml 50 mM $AlCl_3$, 3 x 10 ml distilled water, 3 x 10 ml buffer A (50 mM NH_4OAC, pH 6.0), 3 x 10 ml buffer B (100 mM NH_4OAC and 0.5 M NaCl, pH 7.0), 3 x 10 ml buffer A. The resin was then transferred to a 10 ml disposable column (Bio-Rad). The labeled ,eIF-4E digestion mixture was brought to a total volume of 3 ml with buffer A, the pH was adjusted to 6.0 with concentrated acetic acid, and the sample was

loaded onto the column. To increase the recovery of the labeled peptide the sample tube was washed with 2 ml buffer A. The column was successively eluted with 2 x 10 ml buffer A, 1 x 10 ml buffer B, 1 x 10 ml buffer A, and the radiolabeled peptide was eluted with 6 ml buffer C (10 mM K_2HPO_4, pH 8.0). Chromatography was conducted at room temperature with a flow rate of 0.5 ml/min. All fractions were assayed for radioactivity on a Wallac Model 1409 Liquid Scintillation Counter (99% counting efficiency for ^{32}P).

Reverse Phase High Performance Liquid Chromatography and Amino Acid Sequencing of Photolabeled Peptide: The radioactive fractions resulting from buffer C elution from the aluminum(III)-chelate chromatography were pooled and concentrated in a Savant SVC100H speed vac concentrator until a volume of 1.5 ml was reached. 250 μl samples were then analyzed by reversed-phase HPLC using a microbore C_8 column (Brownlee Lab) and an Applied Biosystems 130A separation system. The mobile system consisted of a 25 μM $AlCl_3$/0.1% TFA solution (X) and a 0.1% TFA/70% acetonitrile (Y) solvent system. The gradient was as follows; 100% X at a flow rate of 50 μl/min for 5 minutes, 0-100%Y at a flow rate of 125 μl/min for 45 minutes, and 100% Y at a flow rate of 125 μl/min for 5 minutes. Photolabeled peptides were detected by exact correlation of absorbance at 220 nm and ^{32}P cpm. Fractions containing photolabeled peptides were concentrated to 20 μl and subjected to amino acid sequence analysis at the Hunter College Sequencing and Synthesis Facility using an Applied Biosystems 477A protein sequencer and an Applied Biosystems 120A analyzer with on-line PTH derivative identification.

Competitive Binding Experiments: The fluorescent m^7GTP cap analog, anthraniloyl-m^7GTP (ant-m^7GTP) was synthesized as previously described (Ren & Goss, 1996). The competitive substitution reactions were performed at constant ant-m^7GTP concentration (1.5 μM) and increasing amounts of 8-azido GTP. The buffer used for all fluorescence measurements consisted of 20 mM HEPES-KOH and 1 mM DTT (pH 7.6). All chemicals were molecular biology grade. Fluorescence measurements were made at 25° C on a SPEX Fluorolog-τ2 spectrofluorometer equipped with a high intensity (450 W) xenon arc lamp. An excitation wavelength of 332 nm was used to monitor the Ant-m^7GTP fluorescence emission at 420 nm. Excitation and emission slit widths of 2.0 mm were used and a 1.0 cm sample cell path length was employed. Lineweaver-Burk plots of $1/\Delta F$ vs 1/[eIF-4E] at varying concentrations of 8-azido GTP will intersect at the same point on the y-axis for competitive inhibition.

Protein Fluorescence Measurements: Fluorescence titration experiments were performed to determine the equilibrium binding constants for the binding of m^7GTP to wild type ,eIF-4E and to the eIF-4E binding site mutants. Fluorescence measurements were made at 25°C on a SPEX Fluorolog-τ2 spectrofluorometer equipped with a high-intensity (450 W) xenon arc lamp. An excitation wavelength of 280 nm was used to monitor the tryptophan fluorescence emission of ,eIF-4E at 330 nm. Excitation and emission slit widths of 1.5 and 2.0 mM, respectively, were used and a 1.0 cm sample path length was employed. The buffer used for all fluorescence measurements was 20 mm HEPES-KOH at pH 7.6 and 1 mM DTT. The steady state data were collected and analyzed as described previously

(Carberry et al., 1989).

Circular Dichroism Measurements: Circular dichroism spectra of FPLC purified eIF-4E proteins were measured on a Jasco-J710 spectropolarimeter. Spectra were obtained in a 0.1 M phosphate buffer at pH 7.6. All measurements were performed using a 0.5 mm pathlength quartz cell at 25 °C. Each sample was scanned 10 times and high frequency noise reduction was applied. Data were recorded at 0.5 mm intervals with a time constant of 1.0 s and 1.0 constant spectral bandwidth.

Preparation of the Binding Site Peptide Column: The storage solution from shipping was allowed to pass through the agarose beads (2 ml) of the AminoLink Plus columns. The column was then equilibrated with 5 ml of enhanced coupling buffer (0.1 M sodium citrate, 0.5 M sodium carbonate, pH 10.0). 2.5 mg 4E peptide was immobilized on the column in 2 ml of enhanced coupling buffer (gel capacity 5-10 mg/ml).The Column was put on a flatbed rocker for 4 hours at 4° C. A second incubation was performed for 4 hours with 5 ml neutral pH coupling buffer (0.1 M sodium phosphate, .015 M NaCl, pH 7.2) under the same conditions. The column was then washed with 3x4 ml wash solution (1 M NaCl) and allowed to sit at room temperature for 2 hours during preparation of the globin mRNA sample.

Binding Site Peptide Column Chromatography: 25 μl of mRNA (890 ng/μl was applied to the column in loading buffer (20 mM HEPES-KOH, pH 7.6). The column was left to

incubate for 1 hour at room temperature, then washed with 10x1 ml loading buffer. No RNA was detected in any of the fractions as observed by DNA DipSticks. The column was washed with 8x1 ml elution buffer (200 mM phosphate, pH 6.2) and the fractions were collected, neutralized with 50 ml of 1 M Tris-KCl buffer,pH 9.0, and analyzed for the presence of RNA.

Chapter 3

The ₚeIF-4E Cap Binding Domain

Identification of the Cap Binding Domain of $_r$eIF-4E Using the Photoaffinity Analog [γ^{32}P]8-N_3GTP

Results

Photoaffinity Labeling of $_r$eIF-4E: The specificity of [γ^{32}P]8-N_3GTP, see Fig. 6, was demonstrated by saturation effects with the probe and by protection studies with m^7GTP, unmethylated nucleotides, and a capped mRNA. Photoinsertion was saturated at 70 μM with an apparent K_d of about 19 μM (Fig. 7). Increasing concentrations of m^7GTP resulted in decreased photoinsertion by [γ^{32}P]8-N_3GTP with more than 75% maximal protection observed at 15 μM m^7GTP with an apparent K_d of 7 μM (Fig. 8). The percent maximal protection by m^7GTP (at 12% [γ^{32}P]8-N_3GTP incorporation) with respect to control (no m^7GTP) is determined by dividing the [γ^{32}P]8-N_3GTP concentration (40 μM) by the total maximum nucleotide plus probe concentration (340 μM). This result provides evidence that photoinsertion of [γ-^{32}P]8-N_3GTP was indeed occurring at the m^7G cap binding site of eIF-4E.

To further study the specificity of photoinsertion of the probe into the m^7G mRNA cap binding site, the ability of other nucleotides and a capped mRNA to prevent [γ^{32}P]8-N_3GTP photoinsertion was studied (Table 2). Among the unmethylated nucleotides, GTP (21% of control), GDP (26% of control), and ATP (36% of control) proved to be the best inhibitors to photoinsertion (where control represents no nucleotide and 100% photoinsertion).

Figure 6. Structure of the photoaffinity probe, [γ-^{32}P]8-N_3GTP which was used in this study to identify the ,eIF-4E cap binding site.

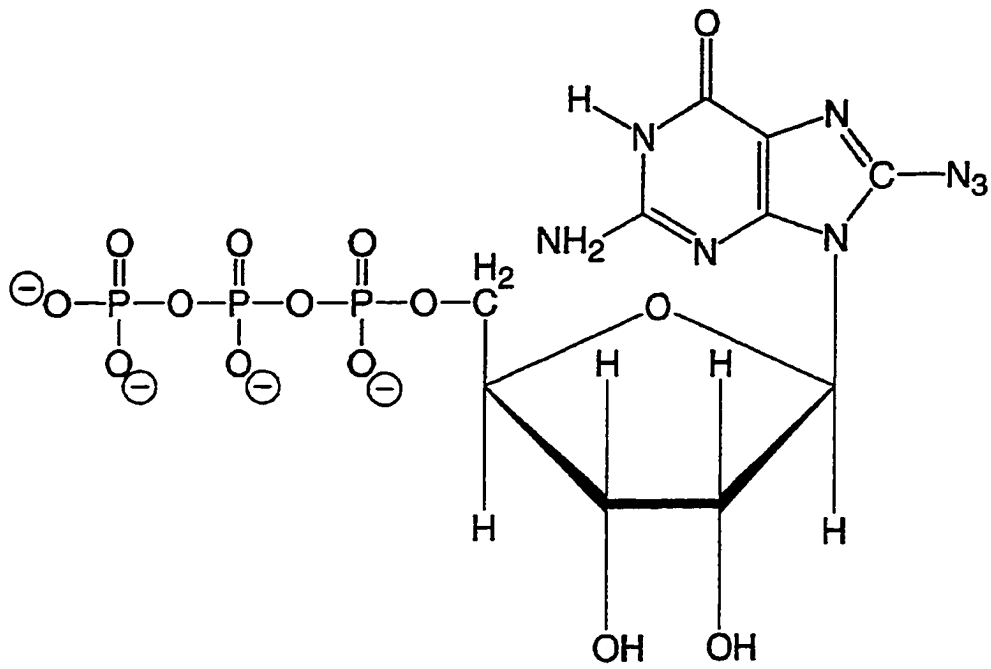

Figure 7. Saturation of [γ^{32}P]8-N_3GTP] photoincorporation into $_r$eIF-4E. $_r$eIF-4E (4 μg) was incubated with the indicated concentrations of [γ^{32}P]8-N_3GTP] under the conditions described in Methods.

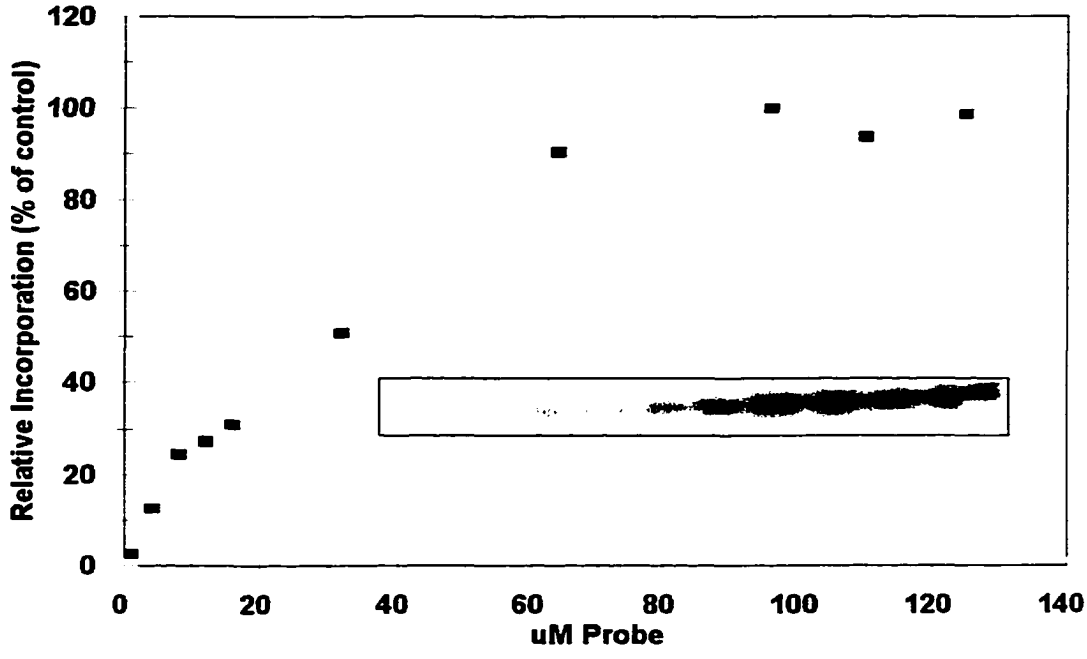

Figure 8. Prevention of [γ^{32}P]8-N_3GTP] photoincorporation into $_r$eIF-4E by m^7GTP. $_r$eIF-4E (4 μg) was incubated with 40 μM [γ^{32}P]8-N_3GTP] in the presence of increasing concentrations of m^7GTP under the conditions described in Methods.

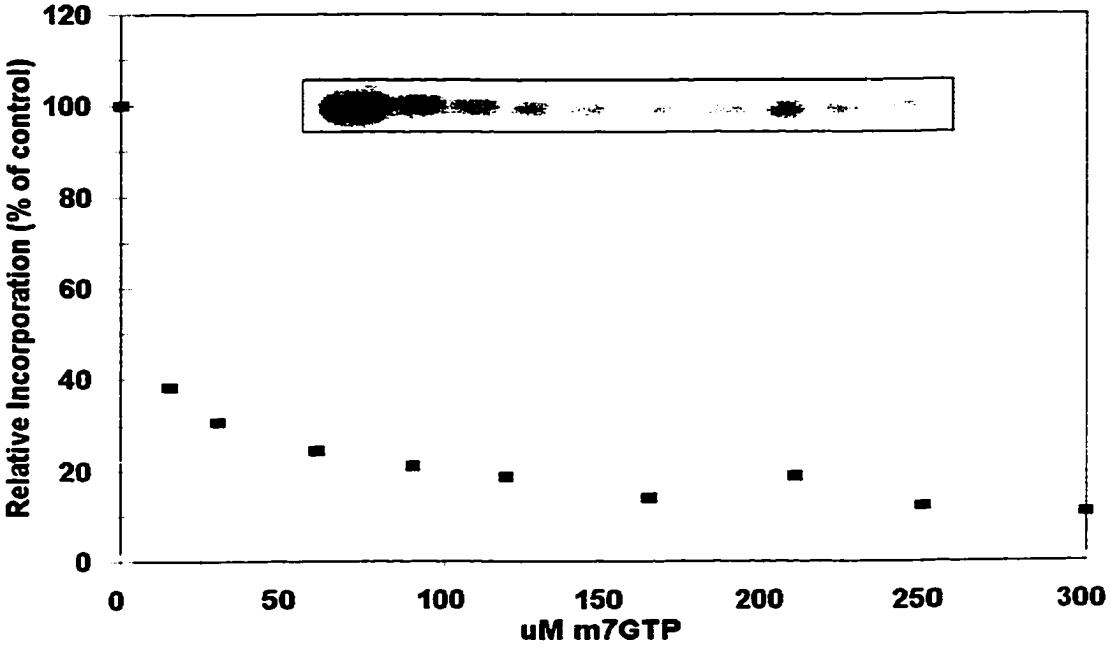

Table 2. Percent of photolabeling of eIF-4E by 40 μM [γ^{32}P]8-N_3GTP in the presence of various nucleotides and capped mRNA

		Photoinsertion
nucleotide	nucleotide concentration	% of control
none	0 μM	100
GTP	300 μM	21
GDP	300 μM	26
GMP	300 μM	73
CTP	300 μM	43
ATP	300 μM	35
ADP	300 μM	51
AMP	300 μM	89
UTP	300 μM	58
UDP	300 μM	93
UMP	300 μM	93
m^7GTP	300 μM	16
capped mRNA[a]	300 μM	5

[a]capped mRNA,34 base long oligoribonucleotide

Although other nucleotides were also able to act as inhibitors they were much less effective. Capped mRNA was able to dramatically reduce photoinsertion (5% of control) as compared to equimolar concentrations of m^7GTP (18% of control) and unmethylated nucleotides (maximum of 21% of control).

The observation that nucleotides other than m^7GTP caused some protection lead to a further determination of azido GTP binding to the active site. A fluorescent derivative of m^7GTP, Ant-m^7GTP, has recently been synthesized in our lab (Ren & Goss, 1996). This probe binds competitively with m^7GTP for the active site. GTP and other nucleotides do not compete for binding. Since this fluorescent probe binds the active site, 8-azido GTP competition was tested with this probe. Fig. 9 shows Lineweaver-Burk plots of the binding. In the case of competitive inhibition, Lineweaver-Burk plots meet at the same Y-axis intercept as is clearly shown in Fig 9.

Isolation and Identification of [γ-^{32}P]8-N_3GTP Photolabeled Peptides: $_r$eIF-4E was photolabeled as described above to determine the amino acid sequence that was covalently modified by [γ-^{32}P]8-N_3GTP within the m^7G cap binding site. The second round of photolysis was performed with nonradioactive 8-N_3GTP to increase the amount of binding domain peptide while reducing nonspecific radiolabeling. TCA was initially used to precipitate photolabeled $_r$eIF-4E, however this approach resulted in low yields of peptide for sequencing, probably due to the disruption of the acid sensitive probe-peptide bond. However, acetone precipitation of photolabeled $_r$eIF-4E resulted in higher yields of labeled

Figure 9. Lineweaver-Burk plot for the competition of Ant-m^7GTP and 8-N_3GTP in binding to $_r$eIF-4E. 8-N_3GTP concentrations are as follows: ●, 0 μM; ▲, 3.4 μM; and ■, 6.4 μM.

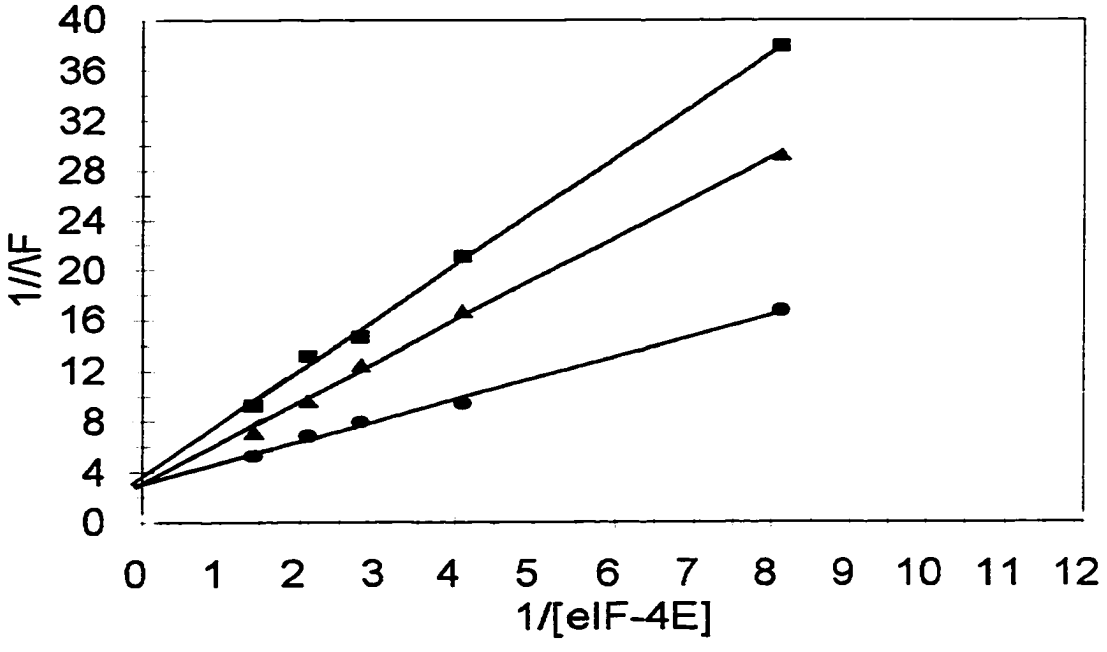

peptide. Photolabeled ,eIF-4E was digested overnight with modified trypsin. The labeled peptide was isolated by affinity chromatography and further purified by reversed-phase HPLC, using the methods described above. To locate the photolabeled peptide in the various buffer solutions the flow through fractions (fractions 1-5), washes (fractions 6-25), and phosphate elutions (fractions 26-31) (Fig. 10) were separately pooled and subjected to reversed-phase HPLC. The flow through and wash fractions contained no radioactive peaks as determined by liquid scintillation counting thus no labeled peptides (data not shown). However, these fractions did contain many peptide fragments, demonstrating that most of the peptides are unmodified and not retained on the Al^{3+} resin. The HPLC absorbance profile at 220 nm and the corresponding ^{32}P cpm profile for the phosphate elution (fractions 16-31) is shown in figure 11. Two major radioactive peaks were observed which also gave a UV absorbance. The first peak at 3 minutes represents the flow through and injection disturbance and contained no peptides as revealed by sequencing data. The radioactivity detected with this peak was free photolyzed [γ-^{32}P]8-N_3GTP, or probe hydrolyzed during HPLC due to the lability of the N-glycosyl bond to acidic conditions (King et al., 1991). The second major radioactive peak at 23 minutes was concentrated for amino acid sequence analysis. Photolabeling, peptide isolation, and sequencing were repeated in three separate experiments to ensure that only one binding domain was covalently modified by [γ-^{32}P]8-N_3GTP. In all experiments the radioactivity coeluted with fraction 23. The sequenced peptide consisted of residues 113-122 of human eIF-4E which includes tryptophan 6 (see Table 3). In addition the lysine residue at position 119 remained uncleaved by trypsin. This information combined with the lack of identification of lysine 119 by sequence analysis

indicates that the residue is the likely site of photoinsertion. No minor peptides were detected in the sequencing data.

Figure 10. Radioactivity profile of immobilized Al^{3+} chromatography of tryptic peptides. Fractions 1-5 represent flow through, 6-25 represent various buffer washes, and 26-31 represent fractions eluted with 10 mM K_2HPO_4. ^{32}P levels were determined with liquid scintillation counting.

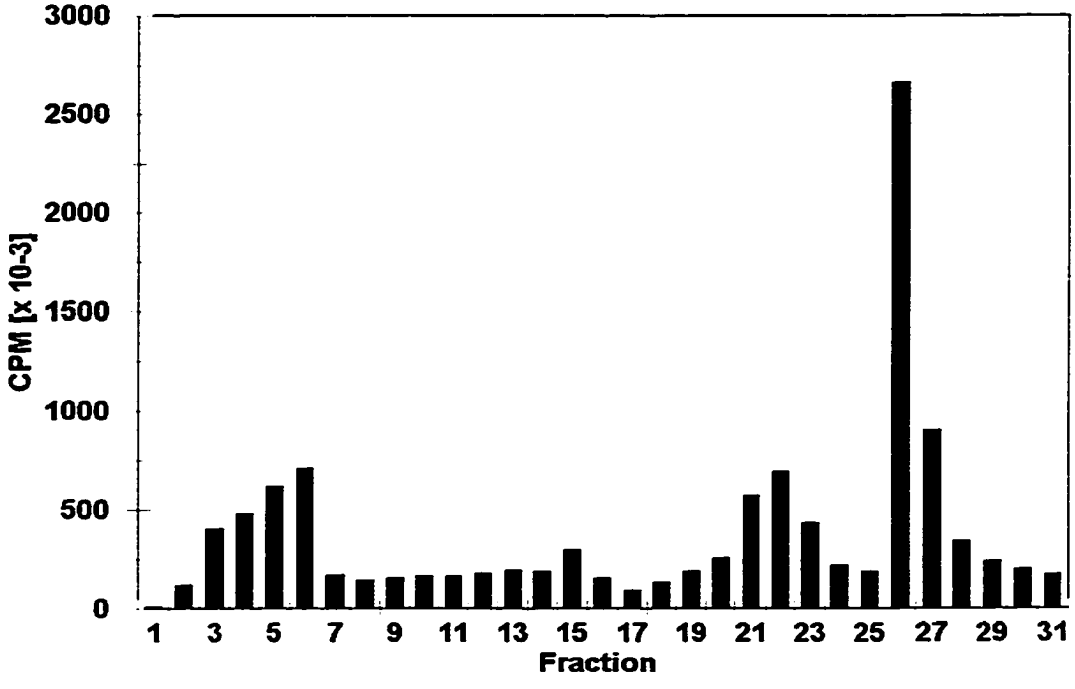

Figure 11. Radioactive profile of microbore, C_8 reverse-phase HPLC of tryptic peptide fractions from Al^{3+} chelate chromatography. (Top): Typical UV profile of the radioactive fractions resulting from K_2HPO_4 elution of the Al^{3+} chelate column. (Bottom): Corresponding ^{32}P profile of the fractions resulting from the HPLC in A. Radioactivity levels were determined by liquid scintillation counting.

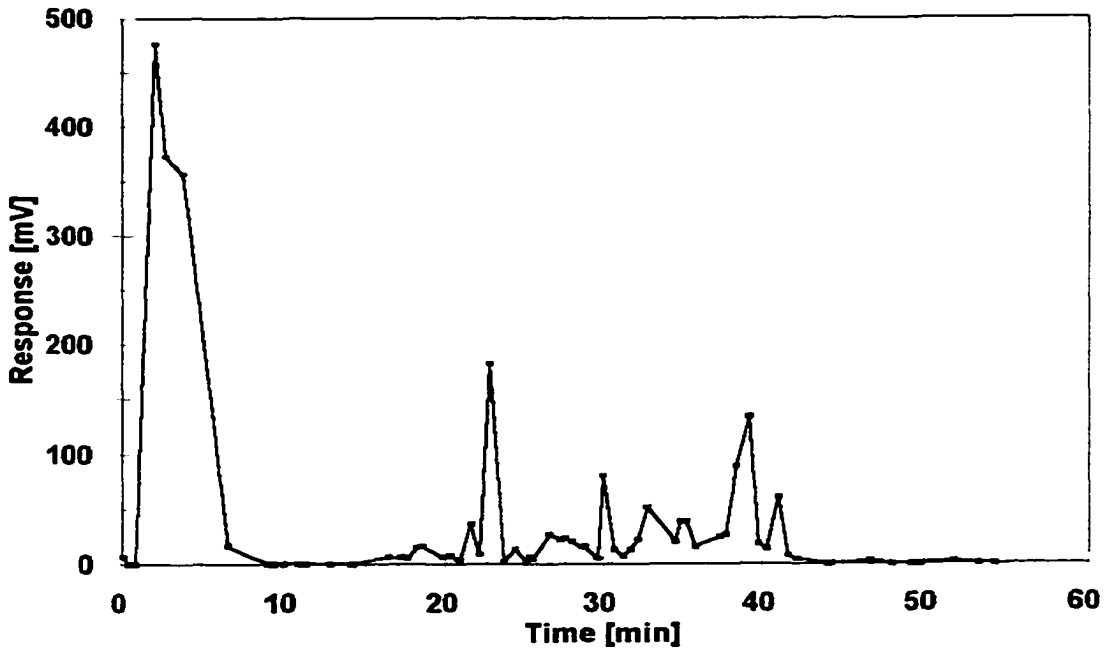

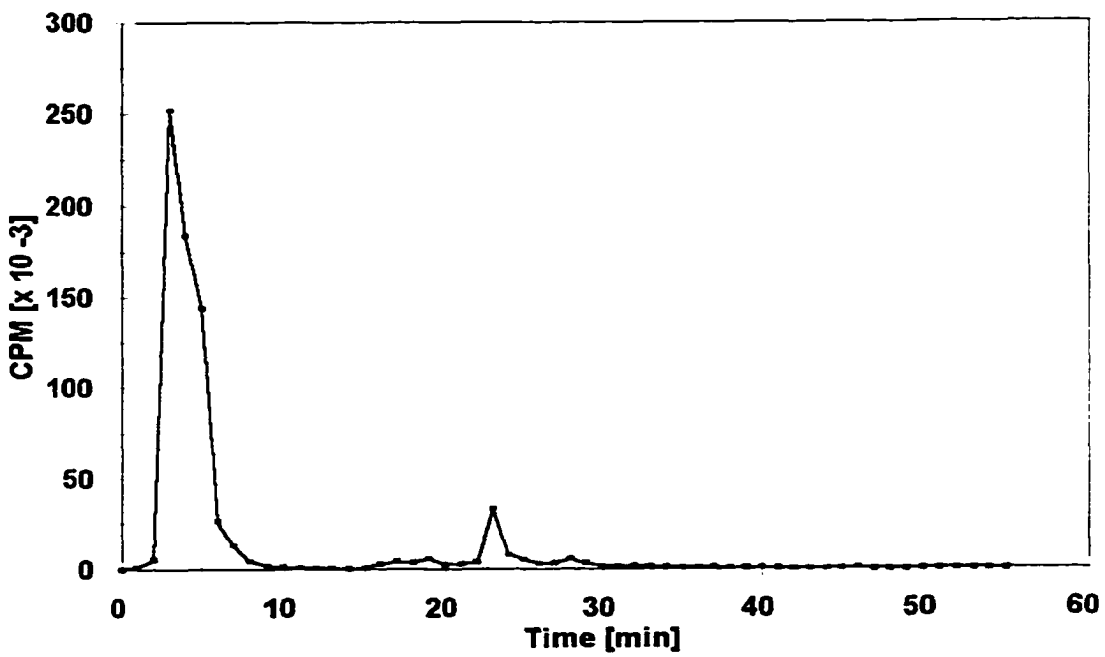

Table 3. Sequence of the [γ-^{32}P]8-N_3GTP photolabeled tryptic peptide from the radioactive peak at 23 minutes in the HPLC chromatogram.

cycle number	identified residue	picomoles observed
1	W	5.6
2	L	17.5
3	I	14.1
4	T	10.6
5	L	11.7
6	N	7.0
7	K	NF[a]
8	Q	6.4
9	Q	4.9
10	R	2.1

[a]NF, not found

Discussion

Binding studies of m^7GTP, m^7GpppG, and various capped mRNA's with eIF-4E have provided insight into the nature of the eIF-4E•cap interaction (Carberry et al., 1992, Carberry et al., 1989, Goss et al., 1990). Tryptophan stacking and hydrogen bonding with glutamic acid residues have been suggested to be important factors (Adams et al., 1978, Isshida et al., 1988, Kamiichi et al., 1987, Ueda et al., 1991b). Additionally, the involvement of a protonated histidine has been proposed (Carberry et al., 1989). These results have allowed for much speculation regarding the specific amino acid residues that constitute the m^7G cap binding site.

The present study demonstrates the ability of [γ-^{32}P]8-N_3GTP to serve as a substitute for the m^7(5')Gppp(5')N cap structure of mRNA in binding to eIF-4E. Selectivity of the probe for the active site was determined in saturation studies with [γ-^{32}P]8-N_3GTP, competitive binding studies with Ant-m^7GTP, and in protection studies utilizing m^7GTP, various nucleotides, and capped mRNA as inhibitors to photoinsertion. Photoinsertion into eIF-4E was saturated with 70 μM [γ-^{32}P]8-N_3GTP and the apparent K_d was 19 μM. The observation that photoinsertion of [γ-^{32}P]8-N_3GTP was inhibited by 90% in the presence of 90 μM m^7GTP demonstrates the specificity of this binding site. The ability of the purine nucleotides GTP, GDP, and ATP to reduce photoinsertion is not surprising because the cap binding site is a dinucleotide site and the probe used in these studies was a mononucleotide. Additional evidence for the site specific insertion of [γ-^{32}P]8-N_3GTP into the cap binding domain is that

of capped mRNA ($m^7G(5')'ppp(5')G$, 34 nucleotides) as the inhibitor which drastically reduced photoinsertion of the probe to 5% of the control (no inhibitor). Competitive binding experiments with Ant-m^7GTP which has been shown to bind the active site give further evidence for site specificity.

The peptide resulting from photoinsertion of [γ-^{32}P]8-N_3GTP and subsequent isolation has been identified as the tryptic peptide consisting of residues 113-122 and thus contains tryptophan 6. Detection of the actual site of nitrene insertion is often difficult due to the lability of the N-glycosyl bond to the acidic conditions of HPLC (King et al., 1991). However these data suggest that lysine 119 is the modified residue for two reasons: the photolabeled binding site peptide is the product of tryptic cleavage at Arg-112 and Arg-122 yet Lys-119 remained uncleaved; and amino acid sequence analysis was unable to identify Lys-119 despite the continuation of sequencing for three residues beyond this position. Such a gap in sequencing usually indicates reaction of the probe with the missing amino acid (Shoemaker & Haley, 1993). The amino acid is "missing" because it does not elute in the expected position when the probe has been covalently attached to it.

Previous fluorescence quenching studies have indicated the involvement of a tryptophan residue (Carberry et al., 1989). Additionally the blue shifted fluorescence emission maximum (330 nm) suggests that the tryptophan resides in a somewhat hydrophobic environment (Carberry et al., 1989). Computer-predicted secondary structure obtained using Chou and Fasman sequence analysis (Chou & Fasman, 1974) indicate that tryptophan 6 comes after a putative turn region and would only be partly exposed (McCubbin et al., 1988).

The calculations also suggest that this residue lies in a region of β-sheet structure. Circular dichroism data from our lab reveals a large conformational transition upon binding of mRNA cap analogues by wheat eIF-(iso)4F. These studies suggest a structural β-sheet interaction motif and that this conformational transition may have a regulatory role (Wang et al., 1995).

Fluorescence and circular dichroism studies have been performed with Trp⇒Lys mutants of tryptophan 6 of yeast eIF-4E which indicate that this residue may be responsible for imparting specificity to cap recognition (McCubbin et al., 1988). It was found that 7-methylated analogs of GDP and G(5')ppp(5')G bind strongly to the mutant, but unmethylated analogs also have binding affinity. The presence of the phosphate groups results in a stacking interaction with the indole ring regardless of the state of methylation. This has been attributed to electrostatic or hydrogen-bonding between the tryptophan side chain and the highly charged phosphates (Kamiichi et al., 1987). The substitution of glycine 111 by aspartic acid in yeast eIF-4E reduced cap binding activity as measured by binding of eIF-4E to m^7GDP agarose affinity columns (Altmann & Trachsel, 1989). This glycine is two residues to the N-terminal side of tryptophan 6.

The identification of residues 113-122 as playing a role in m^7GpppG cap recognition by eIF-4E is consistent with previous studies. The eight tryptophans in yeast eIF-4E have been classified into three separate groups on the basis of the mRNA cross-linking activity of Trp⇒Phe mutants: 1) tryptophans that are strongly required for eIF-4E cross-linking to the mRNA cap which include tryptophans 1,2,5,and 8; 2) tryptophans that reduce the cross-

linking ability of eIF-4E which include 3,6,and 7; 3) tryptophans that are not required for cap recognition which includes 4. Furthermore, the mutation of tryptophans 1 and 8 completely obliterated cap binding activity (Altman et al., 1988). The large number of residues affecting binding may indicate that the overall folding of eIF-4E plays a crucial role in cap recognition. Alteration of the tryptophan residues may interfere with the proposed β-sheet structural motif necessary for binding rather than changing direct base stacking interactions between tryptophan and the m^7G moiety.

Identification of amino acid residues that participate in the $m^7G(5')ppp(5)N$ binding site of eIF-4E will aid in further mutational studies designed to understand the molecular details of eIF-4E•cap recognition. In addition, further knowledge of the structural motif required for eIF-4E•mRNA cap interactions will aid our understanding of precisely how translational repressor 4E-binding proteins function (Lin et al., 1994, Mader et al., 1995).

Subsequent to publication of these data the cocrystal structure and solution NMR structure of eIF-4E bound to m^7GTP was determined (Marcotrigiano et al., 1997, Mausuo et al., 1997). The molecule is shaped like a cupped hand and consists of three alpha helixes and an eight stranded antiparallel beta sheet. Considerable loop closing is evident. The alkylated base is sandwiched between the regions which contain the residues 38-68 and 89-117. This region covers the edge of a central beta sheet. It is sandwiched between the side chains of two conserved tryptophans (Trp-56 and Trp-102). This mode of side chain-base interaction was correctly predicted previously (Ueda et al., 1991a). It is likely that the photoaffinity probe

used in this study crossliked in the region of the eIF-4E cap-binding site where the second nucleotide of a capped mRNA would bind. Lys-119 is two strands away from the primary nucleotide however extensive looping and dynamic breathing modes allow the strands to bring the two nucleotide binding sites in proximity of each other. Recent modeling studies have supported this by showing the m^7Gpp moiety in the region between Trp-56 and Trp 102 and the most favored position for the second nucleotide site is along the edge of a cavity demarcated by Lys-119 and Lys-159 (Spivak-Kroizman et al., submitted).

Chapter 4

Mutants of ₍eIF-4E

Fluorescence and Circular Dichroism Analysis of Mutants of the mRNA Cap Binding Protein, eIF-4E

Results

Fluorescence Spectroscopy Analysis: The preparation of large quantities of recombinant eIF-4E permitted direct determinations of the K_d of binding to the mRNA cap structure and identified N118A, K119A, and Q120A as high affinity mutants. See figure 12 A and B for an example of fluorescence quenching and K_d analysis. Quantitation was performed by measuring the fluorescence quenching of intrinsic tryptophan residues in eIF-4E upon m^7GTP binding at 25°C (Carberry et al., 1989). The curves for fraction protein bound as a function of m^7GTP concentration for wild-type eIF-4E, I115A as one of the lowest affinity mutants, and N118A as one of the high affinity mutants are shown in figure 13. The K_d values of wild-type and mutants of eIF-4E for m^7GTP are shown in table 4. The most notable finding was that the mutants N118A, K119A, and Q120A all had significantly higher binding affinities for m^7GTP as quantitated by the lower K_d, < 0.03 μM, than observed for wild-type eIF-4E (K_d of 1.2 μM). In addition, these mutants (N118A, K119A, and Q120A) did not show an ionic strength dependence on m^7GTP binding (data not shown). Values for R112A and L117A are not reported since data analysis revealed multiple equilibria were present. The quantity of W113A purified was insufficient to quantitate a K_d for m^7GTP due to extremely poor binding of this mutant to the m^7GTP sepharose column during the purification process. Additionally I115A exhibited

Figure 12. (A): Fluorescence quenching curve of 1 μM $_r$eIF-4E as a function of m^7GTP concentration. (B): Eadie-Hofstee plot of the fluorescence changes (ΔF), used to calculate the equilibrium binding constant for the $_r$eIF-4E/m^7GTP complex formation.

Figure 12A

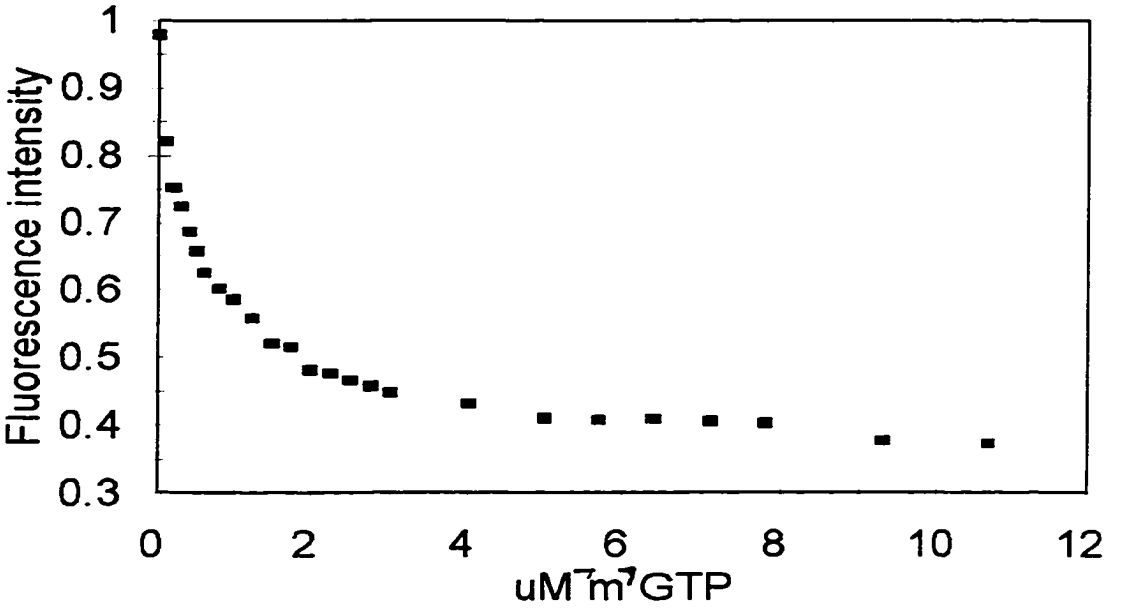

Figure 12B

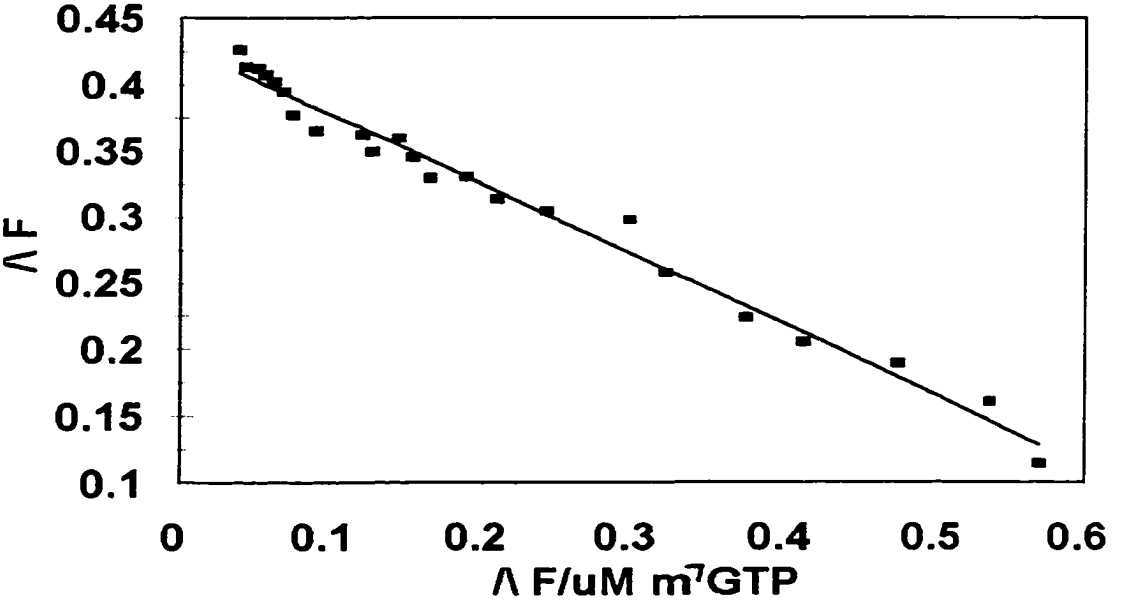

Figure 13. The affinities for m^7GTP of FPLC purified wild-type, I115A, and N118A. The fluorescence intensity of protein as a function of m^7GTP concentration was measured.

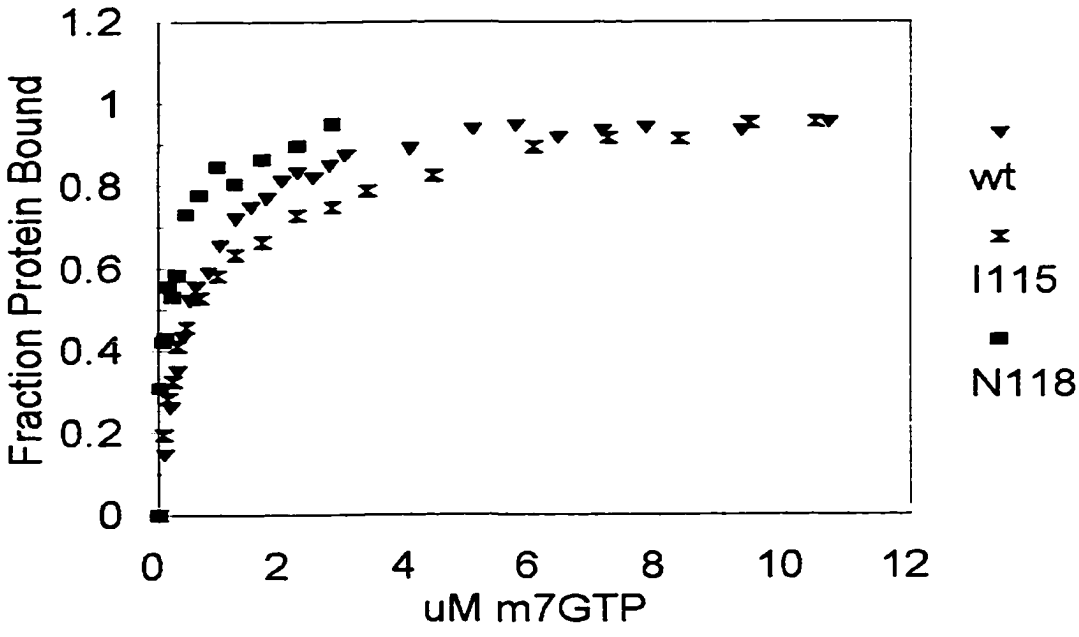

Table 4. K_d's for mutant and wild type $_r$eIF-4E. K_d values were determined from a minimum of three experiments as described in Methods.

r-eIF-4E	K_d (μM)
Wild Type	1.2
R112A	N.D.
W113A	N.D.
L114A	0.8
I115A	2.8
T116A	0.7
L117A	N.D.
N118A	<0.03
K119A	<0.03
Q120A	<0.03
Q121A	1.1

reduced binding as compared to wild-type eIF-4E. Due to the limits in concentration of the proteins, the values for N118A, K119A, and Q120A are reported as upper limits. Errors from data analysis are approximately 15% of the values reported. Replicate experiments differed by about ± 20% of the values reported.

Circular Dichroism Analysis: The structural integrity of the mutant proteins was assessed by a spectral method, circular dichroism (CD). Analysis of I115A, T116A, N118A, and K119A revealed that they were very similar, although not identical, to the wild-type eIF-4E in both free and m^7GTP-bound forms (Figs. 14-17). When spectra for these mutants were fit with the SELCON program for the region 178-250 nm, the estimated percent alpha helix and beta sheet ranged from 18-24% alpha helix and 21-28% beta sheet (Sreerama & Woody, 1993). Among these four mutants K119A was the most different with its unbound form having 18% alpha helix compared to 24% for wild-type and 21% beta sheet compared to 26 % for wild type. CD analysis of R112A suggested that this mutant was less ordered than wild-type eIF-4E. The CD spectra of Q120A suggested that its structure becomes more ordered upon binding to m^7GTP, however, a conformation resembling that of wild-type eIF-4E was not achieved. It was not possible to obtain a CD spectrum of L114A, because it formed a precipitate at the concentrations required for analysis. W113A and L117A were not analyzed because of difficulties in purifying these mutants.

Figure 14. (A): CD spectra for free and m^7GTP-bound wild type eIF-4E. (B): CD spectra for free and m^7GTP-bound R112A mutant eIF-4E.

Figure 15. (A): CD spectra for free and m^7GTP-bound I115A mutant eIF-4E. (B): CD spectra for free and m^7GTP-bound T116A mutant eIF-4E.

Figure 16. (A): CD spectra for free and m^7GTP-bound N118A mutant eIF-4E. (B): CD spectra for free and m^7GTP-bound K119A mutant eIF-4E.

Figure 17. CD spectra for free and m^7GTP-bound Q120A mutant eIF-4E.

Figure 14A

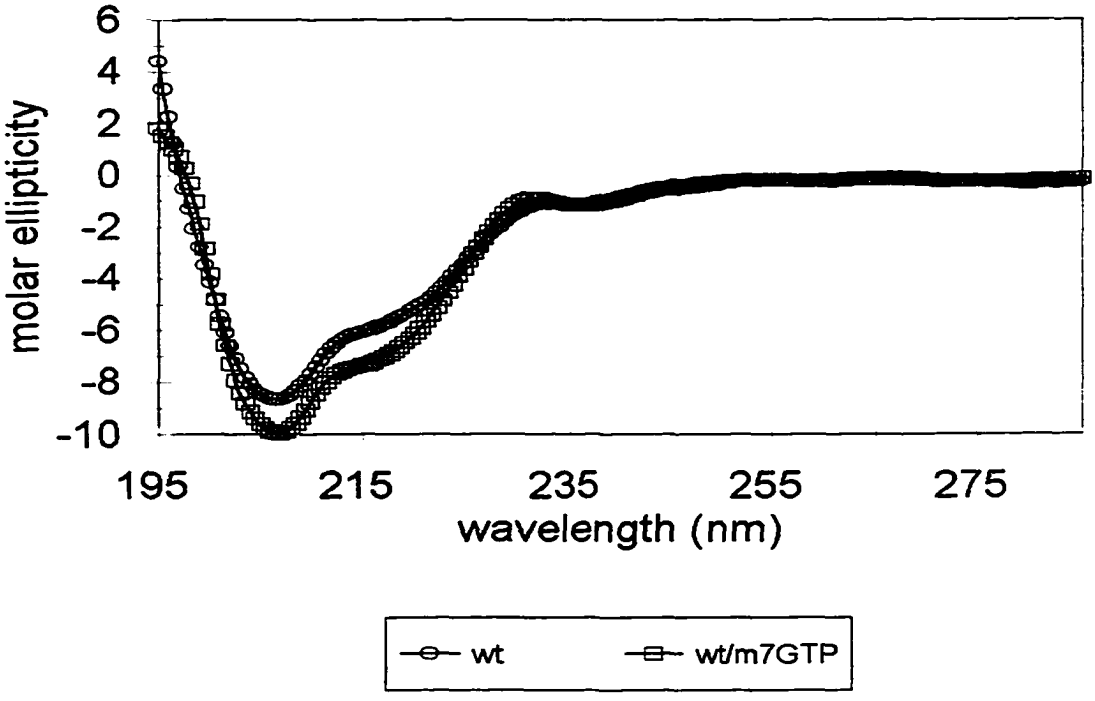

Figure 14B

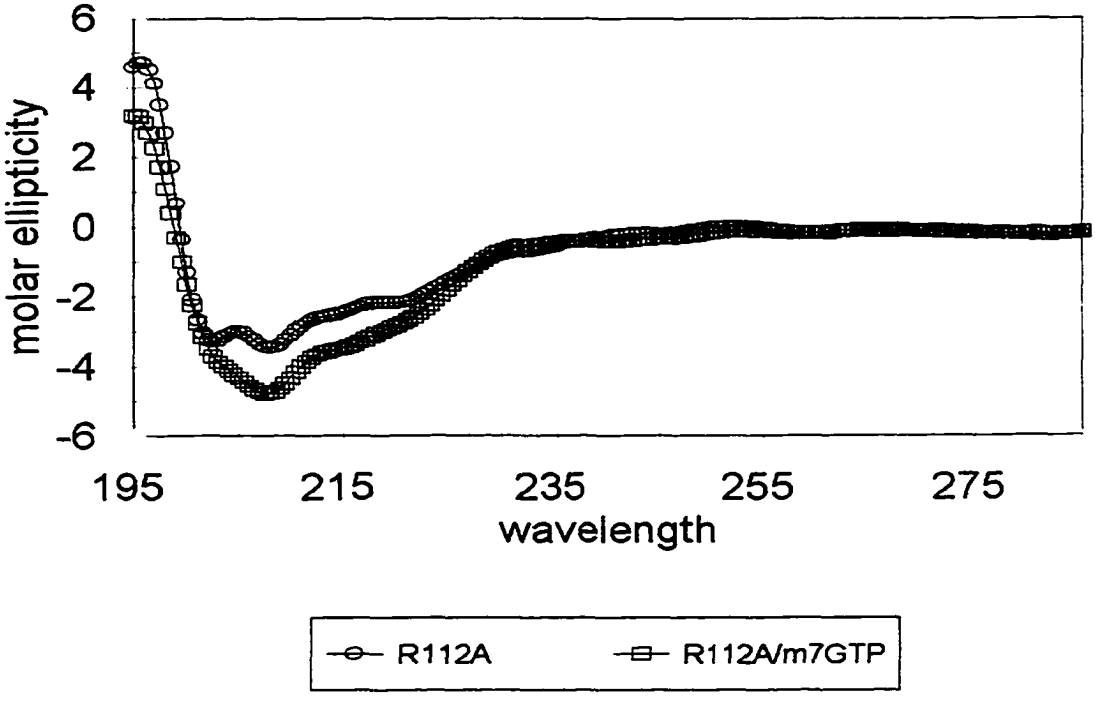

Figure 15A

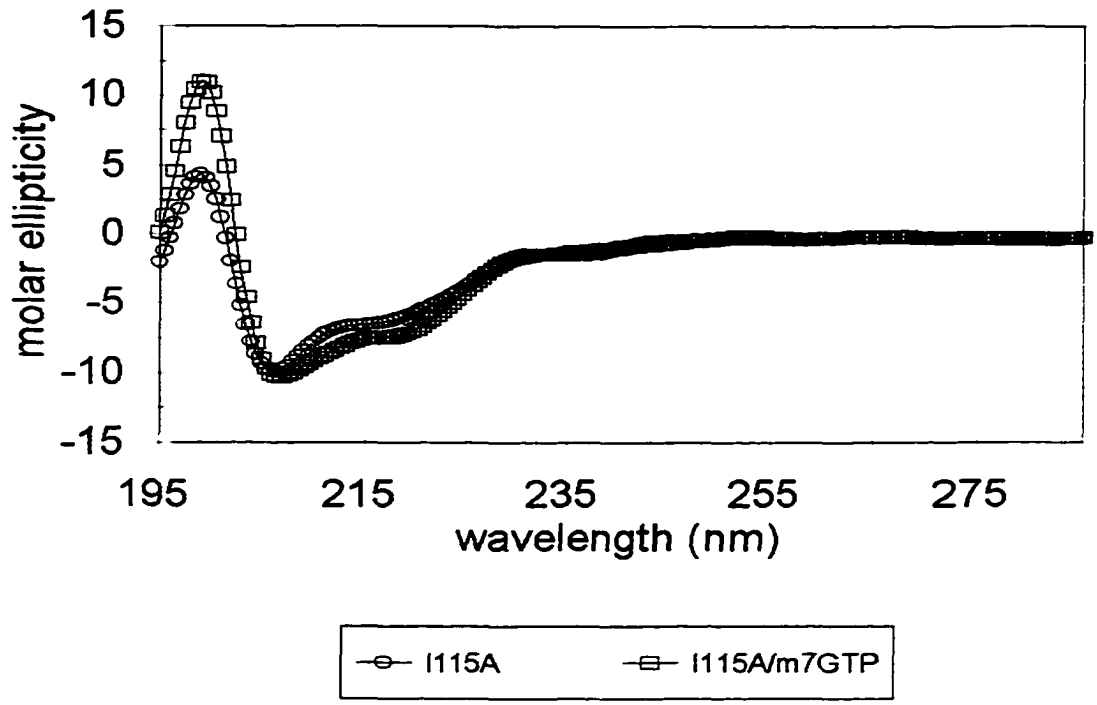

Figure 15B

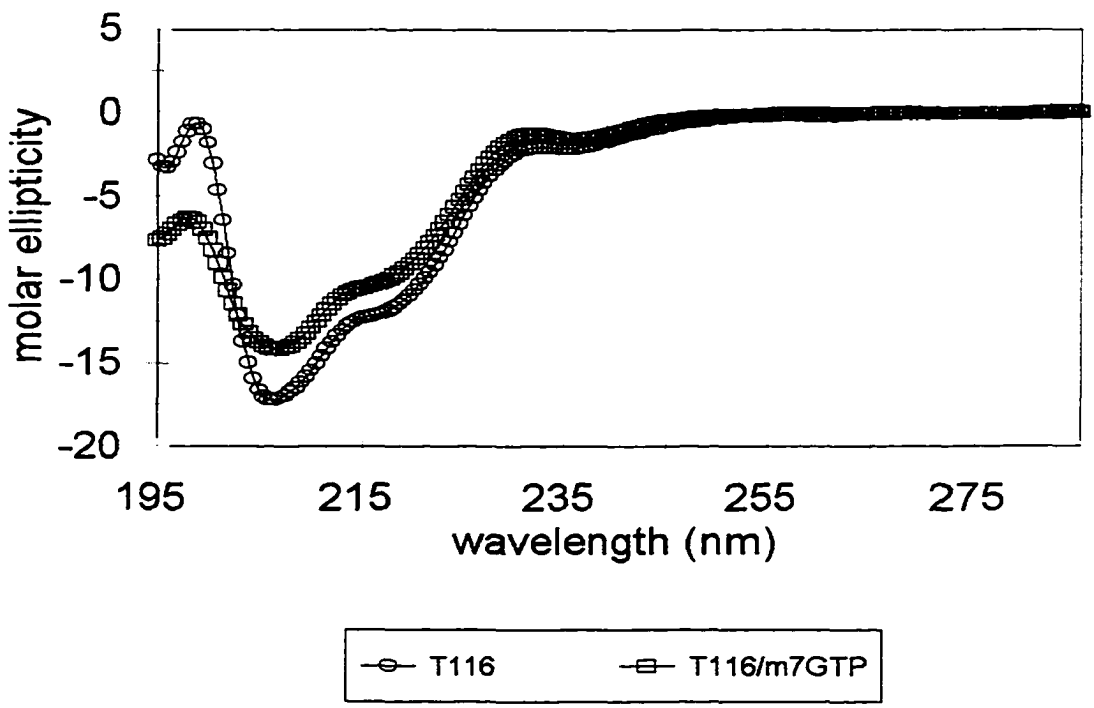

Figure 16A

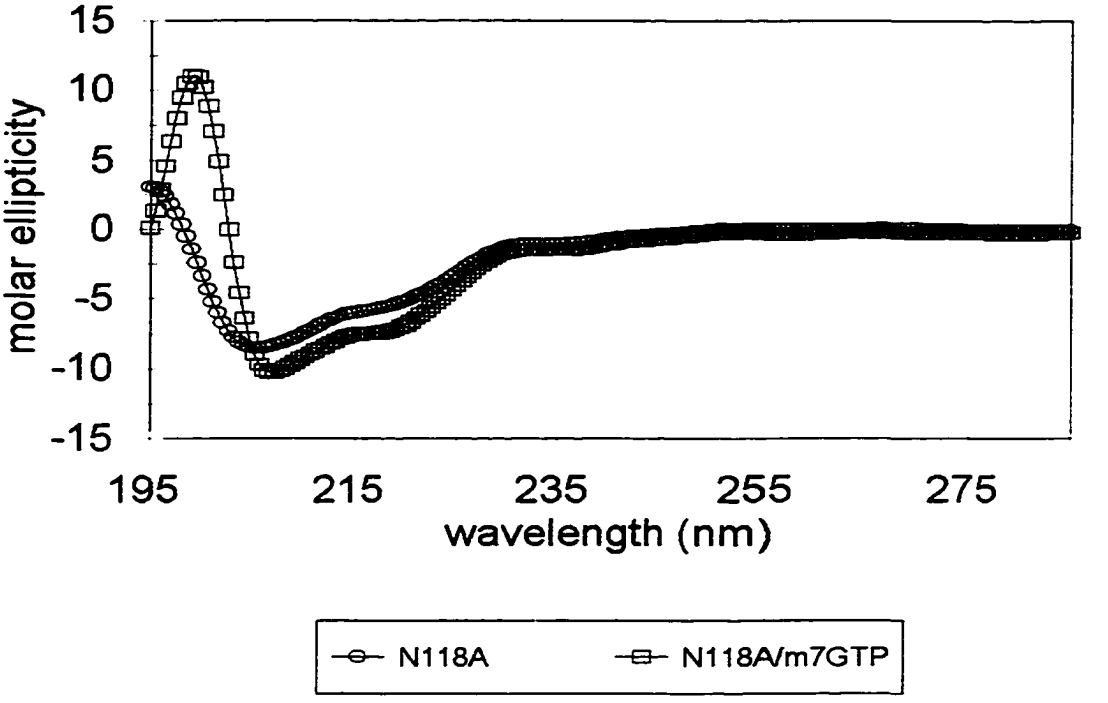

Figure 16B

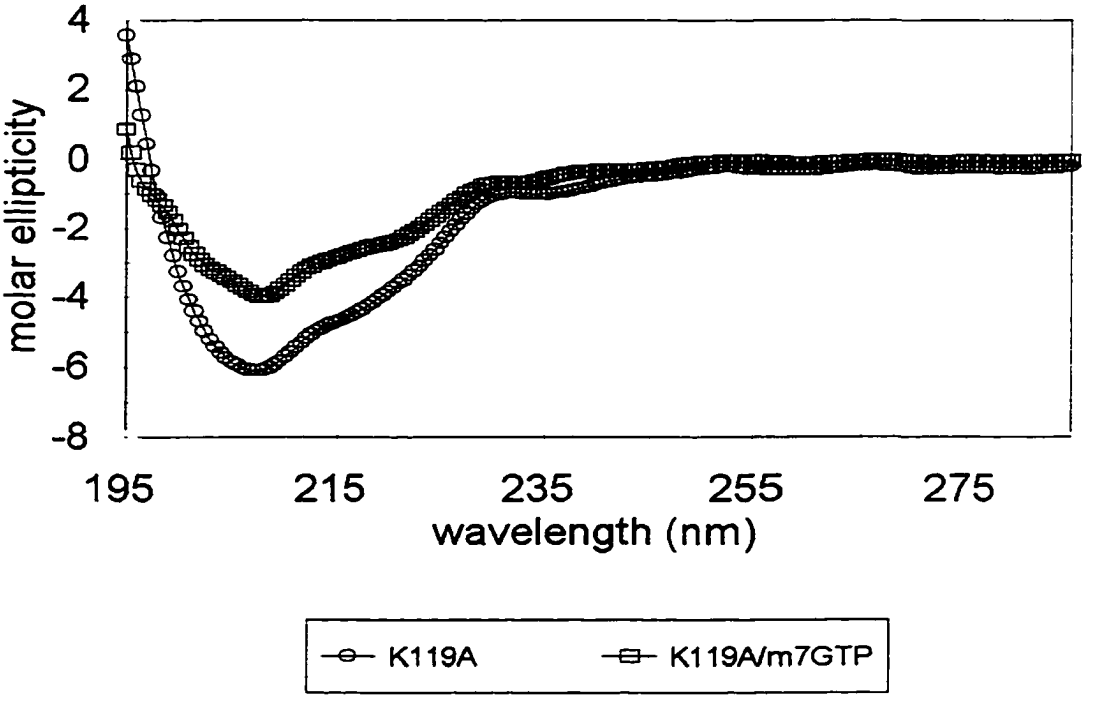

Figure 17

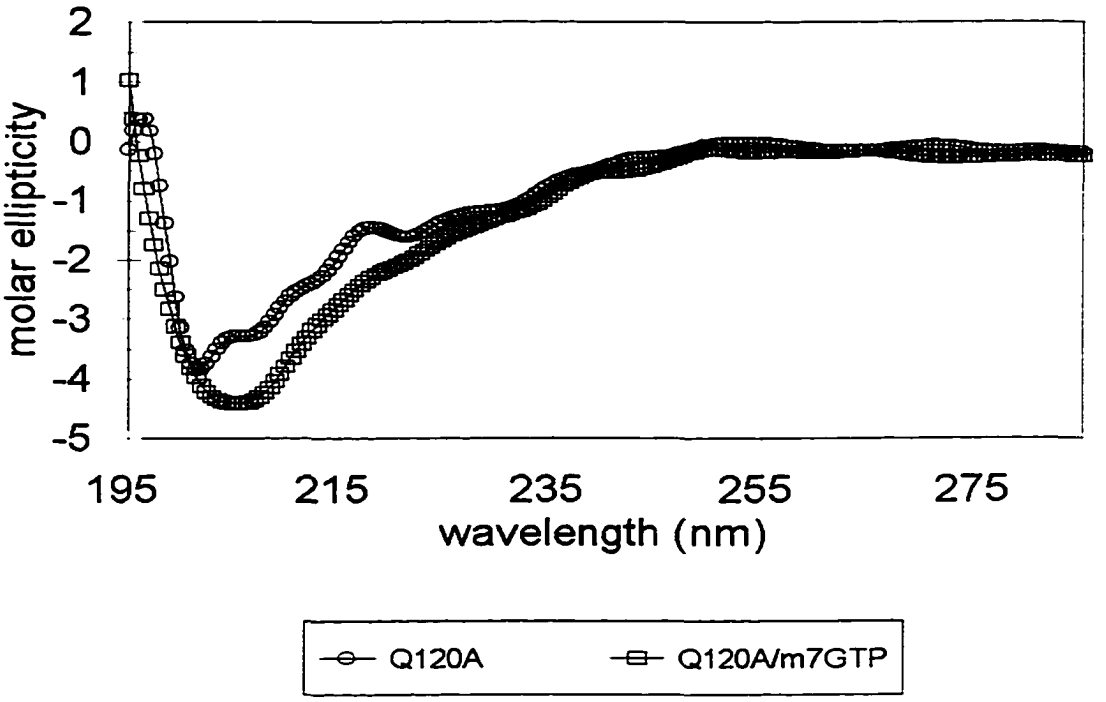

Discussion

The eIF-4E mutants N118A, K119A, and Q120A provide novel examples of eIF-4E which have an affinity for m^7GTP that is up to one order of magnitude higher than wild-type eIF-4E (Table 4). In addition these mutants showed no dependence of m^7GTP on ionic strength as determined by steady state fluorescence spectroscopy which is the same as the observation for wild-type eIF-4E (Carberry et al., 1989). The conformations of these mutants as determined by CD analysis were very similar to that of wild-type eIF-4E. It is possible that the positive charge on Lys-119 repels the positive charge of the m^7GTP purine ring during entrance into its binding pocket. Removal of this charge (K119A) would eliminate the repulsion, creating the observed increase for m^7GTP. In addition, Lys-119 is near Ser-209, the major site of *in vivo* phosphorylation of eIF-4E (Marcotrigiano et al., 1997). Phosphorylation of Ser-209 produces a three to four fold increase in the affinity of eIF-4E for m^7GTP which could be due to a change in the binding site conformation, a change in the breathing modes of the protein, or a change in the local electrostatic potential due to the addition of the negative phosphate group (Minich et al., 1994). A change in conformation might occur following the formation of the proposed salt bridge between PO_4-Ser-209 and Lys-159 which could form a clamp over a bound mRNA (Marcotrigiano et al., 1997). The mutation of Lys-119 to alanine may mimic phosphorylation of Ser-209 through subtle structural changes or by effecting local electrostatic interactions by removing a positive charge. A conclusive answer awaits refinement of the crystal structure which will localize the electron density for the side chain of Lys-119 and Lys-159, or a structure of eIF-

4E/capped RNA or eIF-4E phosphorylated at Ser-209. In addition, the functional analysis of mutants in which Lys-119 and Lys-159 are replaced by negatively charged residues such as Glu may address this question.

Substitution of Trp-113 with alanine dramatically reduced the binding of this mutant to the mRNA cap structure. It is possible this was due to the altered conformation or stability of the mutant. The W113A mutant bound so weakly to m^7GTP sepharose during purification that sufficient quantities of this mutant could not be obtained to measure its K_d for m^7GTP or to perform CD analysis. A similar loss in the ability to bind m^7GTP has been observed when Trp-113 was substituted by Leu, while the more conservative substitution with Phe was less disruptive (Altman et al., 1988, Morino et al, 1996). Moreover, the recent X-ray crystallography model of eIF-4E/m^7GDP positions Trp-113 buried within the protein and part of the hydrophobic core of eIF-4E (Marcotrigiano et al., 1997).

All seven mutants of eIF-4E that had a measurable K_d for m^7GTP were able to support translation of globin mRNA at some level in reticulocyte lysates depleted of eIF-4E (Spivak-Kroizman et al., Submitted). The affinity of I115 for m^7GTP was about half that of wild-type eIF-4E and its structure was similar to wild-type eIF-4E. The lower affinity of I115A was not reflected in the *in vitro* translation assay, and it stimulated globin mRNA translation similarly to wild-type eIF-4E. This is not unexpected in view of the relative inefficiency of cell-free translation systems, particularly those depleted of specific factors, as compared to intact cells. The L117a mutant was not able to support translation in eIF-4E depleted reticulocyte lysates.

L117A may have been unable to initiate translation because of aberrant folding or, alternatively, because other proteins present in the L117A preparation may have inhibited translation.

Chapter 5

Binding Site Purification Column

Preliminary Development and Testing of Binding Site Capped Globin mRNA Affinity Column

Results and Discussion

In order to determine the interaction of the eIF-4E binding site peptide itself (WLITLNKQQR), with m^7GTP direct fluorescence titration experiments were used to measure the equilibrium of binding for the complex. This was done as described in Materials and Methods above, however the emission wavelength in this case was 348 nm. The resulting K_d was .01 μM and thus was substantially tighter than that of wild-type eIF-4E. Thus it was decided that we proceed with preparation and testing of the column.

The peptide column was then prepared as described above and we proceeded to determine whether this would be a viable method for the separation of capped globin mRNA from uncapped RNA which at this time is an extremely expensive venture. Globin mRNA was applied to the column in loading buffer, the column was washed with loading buffer. No free globin mRNA was detected in any of the washes. We then proceeded to determine whether globin mRNA could be subsequently eluted from the column or whether it bound irreversibly. The column was washed with elution buffer and the analysis revealed that the globin mRNA did indeed elute and the highest concentration was found to be in the 6^{th} fraction.

In order to check whether the interaction of RNA with the eIF-4E peptide column was specific rather than ionic, uncapped RNA was submitted to the above protocol. In this instance the RNA eluted with the loading buffer demonstrating specificity of the eIF-4E peptide column for capped globin mRNA.

U.S. Provisional Patent Application number 60-024/881

International Patent Application No. PCT/US97/15295

References

Abramson, R. D., Dever, T. E., Lawson, T. G., Ray, B. K., Thach, R. E., & Merrick, W. C. (1987) *Journal of Biological Chemistry 262*, 3826-3832.

Adams, B. L., M., M., Muthukrishmam, S., Hecht, S. M., & Shatkin, A. J. (1978) *Journal of Biological Chemistry 253*.

Altman, M., Edery, I., Trachsel, H., & Sonenberg, N. (1988) *Journal of Biological Chemistry 263*, 17229-17232.

Altmann, M., & Trachsel, H. (1989) *Nucleic Acids Research 9*, 1643-1656.

Anderssen, L. (1991) *Journal of Chromatography 539*, 327-334.

Carberry, S. E., Friedland, D. E., Rhoads, R. E., & Goss, D. J. (1992) *Biochemistry 31*, 1427-1432.

Carberry, S. E., Rhoads, R. E., & and Goss, D. J. (1989) *Biochemistry 28*, 8078-8083.

Chavan, A. J., Rychlik, W., Blaas, D., Kuechler, E., Watt, D., & Rhoads, R. E. (1990) *Biochemistry 13*, 222-245.

Chou, P. Y., & Fasman, G. D. (1974) *Biochemistry 13*, 222-245.

Donaldson, R. W., Hagedorn, C. H., & Cohen, S. (1991) *Journal of Biological chemistry 266*, 3162-3166.

Duncan, R. F., Milburn, S. C., & Hershey, J. W. B. (1987) *Journal of Biological Chemistry 262*, 380-388.

Goss, D. J., Carberry, S. E., Dever, T. E., Merrick, W. C., & Rhoads, R. E. (1990) *Biochimica Biophysica Acta 1050*, 163-166.

Grifo, H. A., Tahara, S. M., Morgan, M. A., Shatkin, A. J., & Mreeick, W. C. (1983) *Journal of Biological Chemistry 258*, 5804-5810.

Hagedorn, C. H., Spivak-Kroizman, T., Friedland, D. E., Goss, D. J., & Xie, Y. (1997) *Protein Expression and Purification 9*, 53-60.

Hellman, G. M., Chu, L. Y., & Rhoads, R. E. (1982) *Journal of Biological Chemistry 257*, 4056-4062.

Hiremath, L. S., Webb, N. R., & Rhoads, R. E. (1985) *Journal of Biological Chemistry 260*, 7843-7849.

Isshida, T., Doi, M., Ueda, H., Inoue, M., & Scheldrick, G. M. (1988) *Journal of the American Chemical Society 110*, 2286-2294.

Jayaram, B., & Haley, B. E. (1994) *Journal of Biological Chemistry 269*, 3233-3242.

Joshe, B., Yan, R., & Rhoads, R. E. (1994) *Journal of Biological Chemistry 265*, 2979-2983.

Kamiichi, K., Doe, M., Nabae, M., Ishida, T., & Inoue, M. (1987) *J Chem Soc Perkin Trans II*, 1739-1745.

King, S., Kim, H., & Haley, B. (1991) *Methods in Enzymology 196*, 449-466.

Koch, A. E., Cho, M., Burrows, J., Leibovich, S. J., & Polverini, P. J. (1988) *Biochemical, Biophysical Research Communications 154*, 205-212.

Laemmli, U. K. (1970) *Nature 227*, 680-685.

Lamphear, B. J., Kirchweger, R., Skern, T., & Rhoads, R. E. (1995) *Journal of Biological Chemistry 270*, 21975-21983.

Lazaris-Karantzas, A., Montine, K. S., & Sonenberg, N. (1990) *Nature 345*, 544-547.

Lin, T. A., Kong, X., Haystead, T. A., Pause, A., Belsham, G., Sonenberg, N., & Lawrence, C. (1994) *Science 266*, 653-656.

Mader, S., Lee, H., Pause, A., Belsham, G., & Sonenberg, N. (1995) *Molecular Cell Biology 15*, 4990-4997.

Marcotrigiano, J., Gingras, A. C., Sonenberg, N., & Burley, S. K. (1997) *Cell 89*, 951-961.

Matsuo, H., Li, H., McGuire, A.M., Fletcher, M., Gingras, A.C., Sonenberg, N., & Wagner, G. (1997) *Nature Structural Biology*, 717-724.

McCubbin, W. D., Edery, I., Altmann, M., & Sonenberg, N. (1988) *J Biol Chem 236*, 17663-17671.

Merrick, W. C., & Hershey, J. W. B. (1996) *Translational Control*, 31-69.

Metx, A. M., Timmer, R. T., & Browning, K. S. (1992) *Nucleic Acids Research 20.*

Minich, W. B., Balasta, M. L., Goss, D. J., & Rhoads, R. E. (1994) *Proceedings of the National Academy of Sciences, USA 91*, 7668-7672.

Miyage, Y. A. S., Asai, A., Okazake, T., Kuchino, Y., & Kerr, S. J. (1995) *Cancer Letter 91*, 247-252.

Morley, S. J., Rau, M., Kay, J. E., & Pain, B. M. (1993) *European Journal of Biochemistry 218*, 38-48.

Pain, V. M. (1996) *European Journal of Biochemistry 236*, 747-771.

Potter, R., L., & Haley, B. E. (1983) *Methods in Enzymology 91*, 613-633.

Proud, C. G. (1992) *Current Topics in Cell Regulation 32*, 243-369.

Ren, J., & Goss, D. J. (1996) *Nucleic Acids Research 24*, 3629-3634.

Rhoads, R. E. (1988) *TIBS 13*, 52-56.

Rhoads, R. E. (1993) *Journal of Biological Chemistry 268*.

Rozen, F., Edery, I., Meerovitch, K., Dever, T. E., Merrick, W. C., & Sonenberg, N. (1990) *Molecular Cell Biology 10*, 1134-1144.

Rychlik, W., Domire, L., Gardner, P. R., Hellman, G. M., & Rhoads, R. E. (1987) *Proceedings of the National Academy of Sciences, USA 84*, 945-949.

Salvucci, M. E., Chaven, A. J., & Haley, B. E. (1992) *Biochemistry 31*, 4479-4487.

Shoemaker, M. T., & Haley, B. E. (1993) *Biochemistry 32*, 1883-1890.

Sonenberg, N. (1981) *Nucleic Acids Research 9*, 1643-1656.

Sonenberg, S. (1996) *Translational Control*, 245-269.

Sonnenberg, N. (1994) *Biochemie (Paris) 76*, 839-846.

Spivak-Kroizman, T., Friedland, D. E., Xie, Y., De Staercke, C., Goss, D. J., & Hagedorn, C. H. (Submitted) .

Sreerama, N., & Woody, R. W. (1993) *Analytical Biochemistry 209*, 32-44.

Tahara, S. M., Morgan, M. A., & Shatkin, A. J. (1981) *Journal of Biological Chemistry 256*,

7691-7694.

Ueda, H., Iyo, H., Doe, M., Inoue, M., Ishida, T., Morioka, H., Tanaka, T., Nishidawa, S., & Uesugi, S. (1991b) *Federation of European Biochemical Socities Letters 280*, 207-210.

Ueda, H., Iyo, H., Doi, M., Inoue, M., & Ishida, T. (1988) *Biochemical, Biophysical Research Communications 154*, 199-204.

Ueda, H., Iyo, H., Doi, M., Inoue, M., & Ishida, T. (1991a) *Biochimica Biophysica Acta 1075*, 181-186.

Wang, Y., Xiang, T., Sha, M., Balasta, M. L., Friedland, D. E., & Goss, D. J. (1995) *Spectroscopy of biological molecules*.

Webb, N. R., Chari, R. V. J., DePillis, B., Kozarich, J. W., & Rhoads, R. E. (1984) *International Biochemistry 23*, 177-181.

IMAGE EVALUATION TEST TARGET (QA-3)

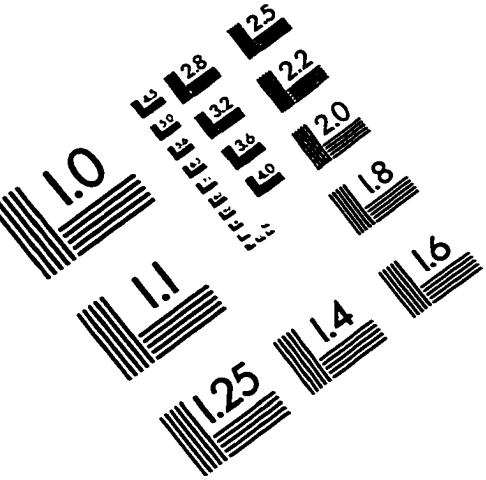

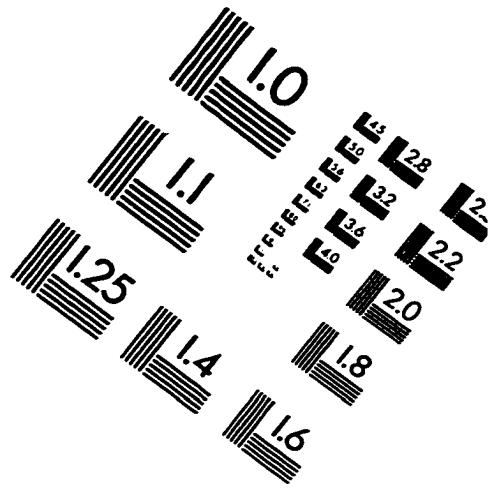

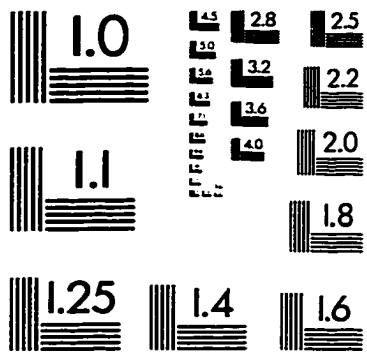

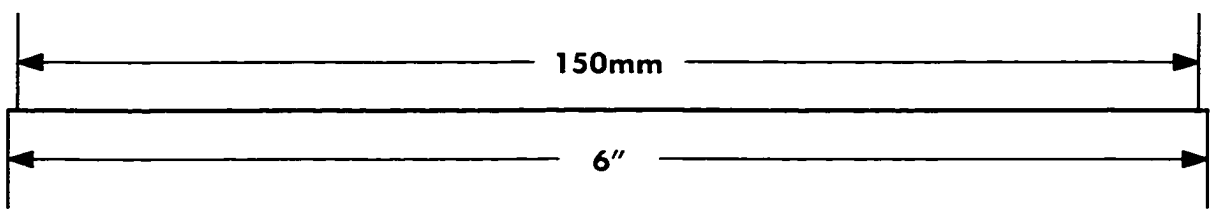

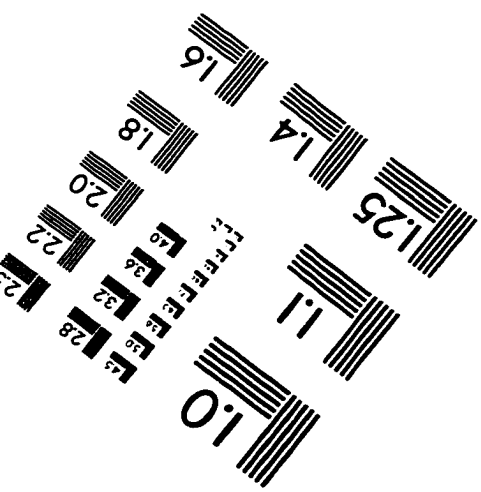

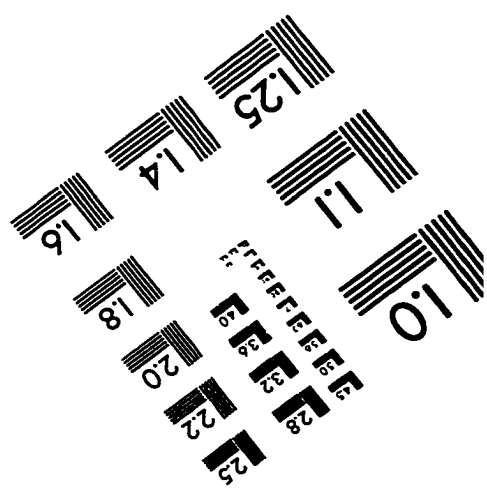

APPLIED IMAGE, Inc
1653 East Main Street
Rochester, NY 14609 USA
Phone: 716/482-0300
Fax: 716/288-5989